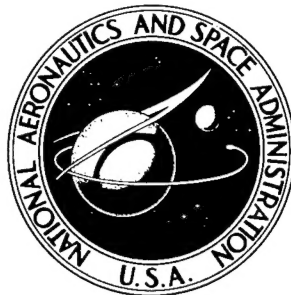


NASA TECHNICAL NOTE

7



033810
B063349
NASA TN D-3243

8

NASA TN D-3243

AMPTIAC

DISTRIBUTION STATEMENT A

Approved for Public Release
Distribution Unlimited

**EXPERIMENTAL INVESTIGATION OF
THERMAL-BUCKLING CHARACTERISTICS OF
FLANGED, THIN-SHELL LEADING EDGES**

by Jerald M. Jenkins and Walter J. Sefic

*Flight Research Center 5
Edwards, Calif. 6*

20020320 220

NATIONAL AERONAUTICS AND SPACE ADMINISTRATION - WASHINGTON, D. C. - JANUARY 1966

10

NASA TN D-3243

EXPERIMENTAL INVESTIGATION OF
THERMAL-BUCKLING CHARACTERISTICS OF FLANGED,
THIN-SHELL LEADING EDGES

By Jerald M. Jenkins and Walter J. Sefic

Flight Research Center
Edwards, Calif.

NATIONAL AERONAUTICS AND SPACE ADMINISTRATION

For sale by the Clearinghouse for Federal Scientific and Technical Information
Springfield, Virginia 22151 - Price \$2.00

EXPERIMENTAL INVESTIGATION OF THERMAL-BUCKLING CHARACTERISTICS
OF FLANGED, THIN-SHELL LEADING EDGES

By Jerald M. Jenkins and Walter J. Sefic
Flight Research Center

SUMMARY

The thermal-buckling behavior of a wide range of flanged, thin-shell leading-edge specimens was investigated. Specimens of varying geometry were subjected to temperature-rise rates up to 50°F per sec (27.7°K per sec) and maximum heating rates up to $19.6\text{ Btu/ft}^2\text{-sec}$ (222.4 kW/m^2). The specimens investigated were constructed of 2024-T3 aluminum, SAE 4130 steel, or Inconel X-750. Regions of stable structural behavior were established on the basis of leading-edge dimensional and thermal-load parameters. Two types of buckling were observed in the flanges of most of the specimens. The results of the experiments provide thermal-buckling information from which a variety of flanged, thin-shell leading-edge geometries may be selected that are free of unstable structural behavior while under the influence of severe thermal loadings.

INTRODUCTION

The leading edges of winged hypersonic aircraft are known to be subjected to intense aerodynamic heating (ref. 1) in flight. Detailed research investigations into specific types of leading edges suitable for hypersonic use have been limited. The heat-sink concept, although excessive in weight and limited to short durations of heating (ref. 2), has been the most widely used type of leading edge for hypersonic application. Limited experimental and analytical work on shell types of leading edges (refs. 3 and 4) has been conducted; however, the thermal-buckling behavior of leading edges has been defined only in analytical studies, such as references 5 and 6. These theories include simplifying assumptions, which impose limitations on their applicability to design problems.

A series of experimental investigations into the thermal-buckling behavior of flanged, thin-shell leading edges has been conducted at the NASA Flight Research Center, Edwards, Calif. Three dimensional parameters were investigated: the shell radius, the flange depth, and the sheet thickness. The experiments included specimens constructed of three metal alloys of differing material properties: 2024-T3 aluminum, annealed SAE 4130 steel, and heat-treated Inconel X-750.

The results of these experiments are presented in this paper to provide information useful in establishing a leading-edge geometry free of thermal-buckling problems. In addition, an insight is offered into the manner in which failure occurs and the severity of the failure.

SYMBOLS

The units used for the physical quantities in this paper are given both in the U.S. Customary Units and in the International System of Units (SI). Factors relating the two systems are given in reference 7.

| | |
|--|---|
| a, b, c | chordwise distance from leading edge to thermocouples 3, 4, and 5, respectively |
| a_1, a_2, a_3 | arbitrary constants |
| d | flange depth, in. (cm) |
| $\frac{d}{t}$ | flange parameter |
| r | inside leading-edge radius, in. (cm) |
| T_f | stagnation-line-failure temperature, °F (°K) |
| ΔT_f | incremental rise above room temperature (80° F (300° K)) at failure, °F (°K) |
| T_m | maximum experimental temperature, °F (°K) |
| t | sheet thickness, in. (cm) |
| x, y | rectangular coordinates |
| α | coefficient of thermal expansion, in./in.°F (cm/cm°K) |
| $\alpha \Delta T_f \left(\frac{d}{t} \right)^2$ | buckling parameter |

DESCRIPTION OF APPARATUS

Eighteen 4130 steel, 15 Inconel X-750, and 18 2024-T3 aluminum flanged, thin-shell leading-edge specimens were fabricated from standard sheet material. Four typical specimens are shown in figure 1. The geometry of the specimens is shown in figure 2(a), and the dimensions are presented in table I. The length of all the specimens was 16.0 inches (40.6 cm), and the taper angle was

constant at 15° (0.262 rad); however, the inside leading-edge radius r , the flange depth d , and the sheet thickness t were all retained as dimensional parameters. The range of variation of these parameters was:

$$t = 0.020 \text{ in. (0.051 cm) to } 0.080 \text{ in. (0.203 cm)}$$

$$r = 0.25 \text{ in. (0.64 cm) to } 1.00 \text{ in. (2.54 cm)}$$

$$d = 2.20 \text{ in. (5.59 cm) to } 5.00 \text{ in. (12.70 cm)}$$

The sheet material for the specimens was first sheared to proper size, then the bend was formed to the designated taper angle. Channels of the same material were formed with 1.00-inch (2.54-cm) flanges to dimensions such that the channel would fit precisely inside the bottom of the leading-edge specimen. A channel 0.080-inch (0.203-cm) thick was constructed for each specimen. Each leading edge was then resistance-welded to its corresponding channel at intervals of 0.5 inch (1.27 cm) along the entire length of the flanges. When the welding operations were completed, the Inconel X-750 specimens were given a full heat treatment (ref. 8). No visible warping or distortion resulted from the treatment.

Prior to the experiments, each of the specimens was instrumented with externally mounted chromel-alumel thermocouples (fig. 2(b)). The specimens were then attached to a beam (figs. 2(c) and 3) by inserting bearing plates inside the specimen and passing symmetrically positioned stainless-steel bolts through the bearing plate, through the web of the channel, and finally through the flange of a stiff beam. The restraining beam was an American Standard 4I7.7 steel beam modified by milling off the outside 0.4 inch (1.02 cm) of the top of the flanges of the beam (fig. 2(c)). The specimens were then striped with high-temperature white paint. Banks of

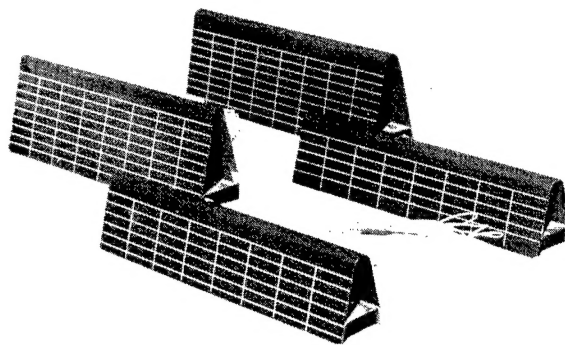
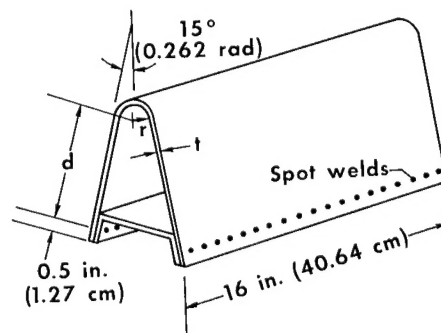
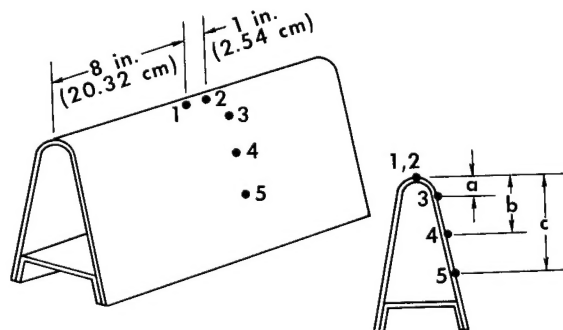


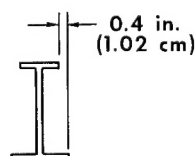
Figure 1.— Four typical flanged, thin-shell leading-edge specimens.



(a) Specimen geometry.



(b) Thermocouple location.



(c) 4I7.7 restraining beam.

Figure 2.— Sketches showing leading-edge-specimen geometry, thermocouple location, and restraining beam.

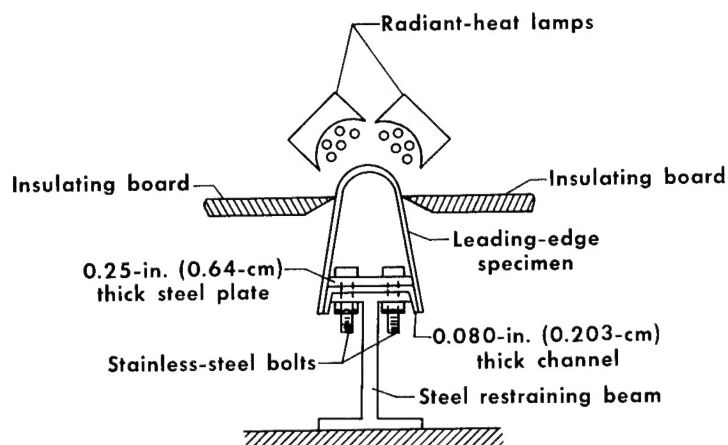


Figure 3.— Sketch of test condition.

radiant-heat lamps were arranged about the upper 1.00 inch (2.54 cm) of the specimens (fig. 3). The banks of lamps overlapped the ends of the specimen to assure uniform heating along the length of the specimen. External heat transfer was allowed only on the radial portion of the specimen and, in some cases, on a small part of the flange of the leading edge. The remainder of the specimen was protected from radiant heat by sheets of high-temperature insulation.

PROCEDURE

A control thermocouple was positioned on the stagnation line of the cylindrical part of the leading-edge specimen 8 inches (20.32 cm) from each end. The heating of the specimen was controlled by this thermocouple. The temperature along the stagnation line of the specimen was programed to rise from room temperature at a rate of 50° F per sec (27.7° K per sec) to 700° F (645° K) for the aluminum specimens, 1200° F (922° K) for the steel specimens, and 1700° F (1200° K) for the Inconel X-750 specimens. The temperatures were held at these respective levels for 10 seconds. The programed temperature time history of the stagnation line of the specimens is shown in figure 4. Four additional thermocouples were installed on all specimens to monitor chordwise temperature

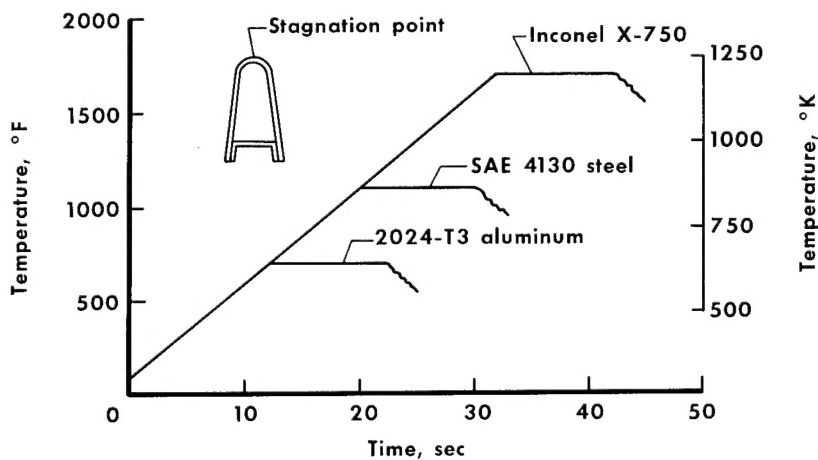


Figure 4.— Programed temperature time histories for specimen stagnation line.

gradients. Table II lists the locations of the thermocouples shown in figure 2(b). Temperatures were recorded on conventional strip-chart recorders with an overall accuracy of ± 1 percent of full-scale deflection of 2400°F (1590°K).

The experiment was started by heating the specimen according to the programmed temperature time history. Two observers were required during the experiments: one visually monitored the behavior of the specimen, and the other noted the time and temperature at which pertinent events occurred. At the conclusion of each experiment, the events were logged, summarized, and classified by the observers.

RESULTS

The most important single observation made during the heating of the leading-edge specimens was whether buckling did or did not occur. In addition, the following items were determined during the experiments:

1. The manner in which buckling occurred.
2. The temperature at which initial buckling occurred.
3. The severity of buckling.
4. The temperature distribution of the specimen.

Table III summarizes the results of the experiments for each of the specimens in terms of either unstable (specimen buckled) or stable behavior (specimen did not buckle). Two modes of unstable behavior were observed (fig. 5). Mode I occurred in the central regions of the flanges of the leading-edge specimen. This mode of buckling was either a single- or multiple-wave pattern similar to the buckling pattern of a plate compressed in one direction with some restraint on all edges. A typical example of this type of buckling pattern can be seen clearly in figure 6 by placing a straightedge along the longitudinal grid lines painted on the flange of the specimen. Mode II buckling also occurred in the flanges of the specimen. This mode of buckling was a single-wave pattern similar to that occurring in a compressed, thin column. An example of this type of buckling is shown in figure 7.

The severity of the buckling and the stagnation-line temperature at which buckling occurred is shown in table III.

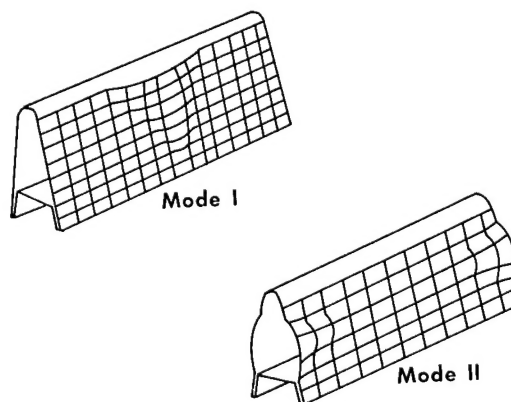


Figure 5.— Buckling modes.

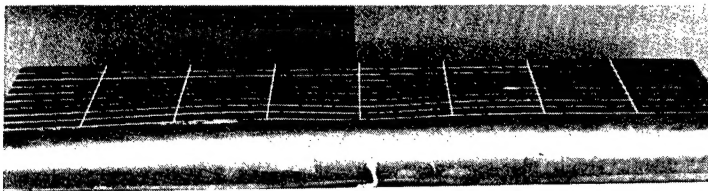


Figure 6.— Example of a Mode I buckle.

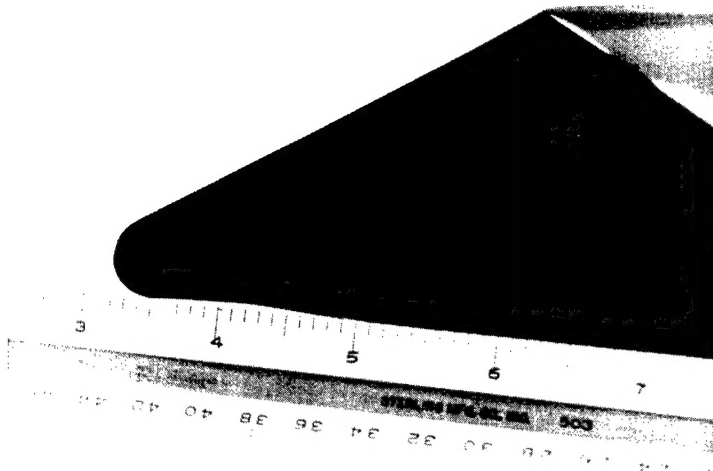


Figure 7.— Example of a Mode II buckle.

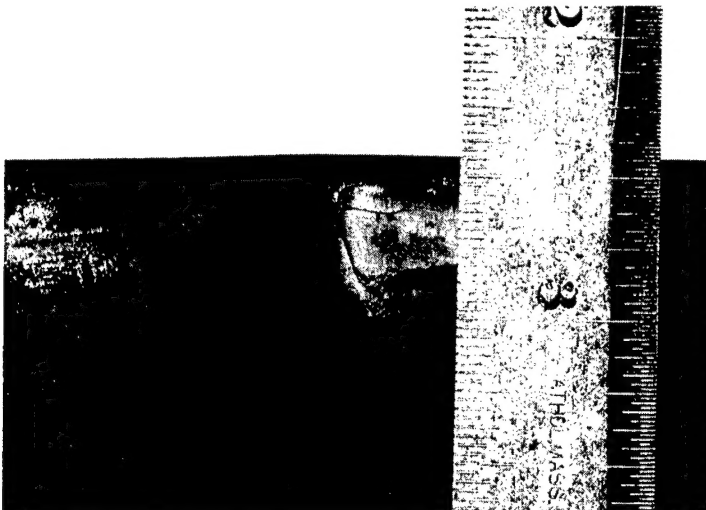


Figure 8.— Example of a cracked specimen.

The severity of buckling was categorized as follows:

None - Buckles were not observed during or after the test.

Moderate - Buckles were almost undetectable by visual observation.

Severe - Buckles were obvious by visual observation.

Gross - Buckles were of such severity that the specimen was essentially incapable of carrying external load.

The temperatures recorded in the stable-behavior column of the table indicate the maximum stagnation-line temperature that the specimen experienced without buckling.

Two of the 51 specimens cracked. The cracks occurred on the flange of the specimen near the radial part (fig. 8). In both instances, a single crack started at a point of severe buckling and propagated in several directions after the heating was stopped.

Chordwise temperature profiles of a typical specimen are shown in figure 9 at 5-second intervals up to the time of maximum temperature. The temperature time histories of all specimens are presented in table IV for 5-second increments.

DISCUSSION OF EXPERIMENTS

The large chordwise temperature gradients and the nonlinear temperature distribution imposed on the specimens during these experiments represent a more severe operating environment than would be encountered by a hypersonic aircraft during actual flight. In addition, the restraining-beam system used to retard thermal bending of the specimens during the experiments provided a stiffer restraint than would normally be required. An unrestrained leading edge is subjected to only first-order (loads arising from non-uniform temperature fields) thermal loads, whereas the introduction of restraint, such as that provided by the restraining beams, leads to zero-order (loads arising from nonuniform thermal action on the mutually connected bodies of a structural system) thermal loads (ref. 9). The presence of both zero and first-order thermal loads represents a combined thermal loading on the leading-edge specimens. Hence, the experimental data were obtained for an extreme thermal-loading environment. If the results are applied to leading-edge geometries within the limitations of this investigation in which the combined thermal loadings are less severe, the data presented represent useful information for design purposes. The computation of the exact stress distribution and the theoretical buckling stress of the specimens is beyond the scope of this paper.

Mode II was the most frequently observed type of buckling during the experiments, as is shown in the following table:

| | Material | | | Total |
|--------------|------------------|------------|---------------|-------|
| | 2024-T3 aluminum | 4130 steel | Inconel X-750 | |
| Mode I | 1 | 2 | 0 | 3 |
| Mode II | 8 | 5 | 8 | 21 |
| Simultaneous | 3 | 5 | 3 | 11 |
| None | 6 | 6 | 4 | 16 |

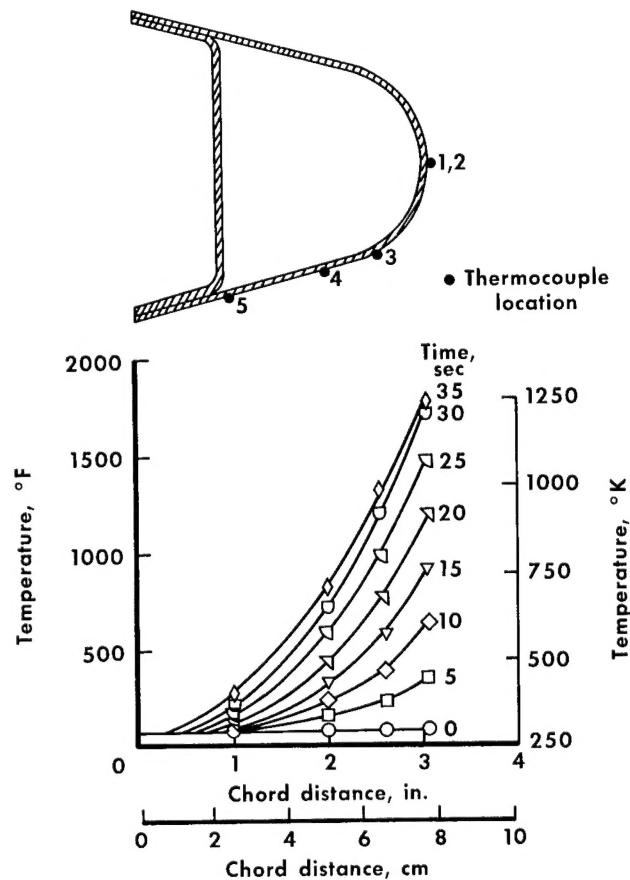


Figure 9.— Chordwise temperature distributions at 5-second increments for a typical specimen (number 50, Inconel X-750).

The large number of Mode II buckles appears to be a logical result, considering the reduced buckling strength that would be associated with the free edge of the specimen flange. Mode I buckling was observed singularly in only three specimens; however, the occurrence of simultaneous buckling of both modes was more frequent. Buckling did not occur in the radial or curved portion of the specimens. Only two of the specimens cracked. Both of these instances involved combined gross Mode I and Mode II buckling, and the crack started after the buckling. Initially, the cracks were very small, but, as the specimen cooled upon completion of the test, the cracks propagated in several directions. This delayed reaction is attributed to residual tensile stresses resulting from compressive yielding during the test.

The most severe buckling occurred frequently on specimens with small thickness. Nine of the 11 occurrences of gross buckling involved specimens with a thickness less than 0.025 inch (0.064 cm). The results of the tests indicate that the severity of buckling increased as the leading-edge thickness decreased.

The effect of specimen thickness on buckling behavior is shown in the following tabulation:

| Thickness, in. (cm) | Number of stable specimens | Total number of specimens |
|--------------------------------|----------------------------|---------------------------|
| 0.078 (0.198) to 0.080 (0.203) | 11 | 11 |
| 0.062 (0.157) to 0.063 (0.160) | 4 | 4 |
| 0.040 (0.102) | 1 | 19 |
| 0.020 (0.051) to 0.025 (0.064) | 0 | 17 |

As can be seen, the maximum temperatures selected for the experiments were insufficient to initiate buckling in specimens having a thickness equal to or greater than 0.062 inch (0.157 cm). However, it is unlikely that the materials investigated would be desirable for use as thin-shell leading edges at temperatures above the maximum values selected for the experiments, since the elastic moduli and yield strength of these materials degrade rapidly above these temperatures. Although the data obtained were insufficient to determine the actual failure temperatures of the specimens having thicknesses in excess of 0.062 inch (0.157 cm), the knowledge that these specimens did not buckle is of considerable practical value.

The specimen length of 16.0 inches (40.6 cm) was selected for two reasons: (1) it was compatible with the lengths of the radiant-heat lamps, in order to assure uniform heating of the specimen in the lengthwise direction, and (2) it was of such magnitude that a significant part of the specimen was essentially free of lengthwise thermal-stress end effects, i.e., the lengthwise first-order

thermal loads in the central regions of the specimen would approach the values of an infinitely long leading edge.

Except for the single interior channel at the base of the leading-edge specimen, no other interior or end stiffeners were used. It was decided that excessive stiffening of the specimens would introduce geometric discontinuities that would unnecessarily complicate the interpretation and analysis of the experimental results.

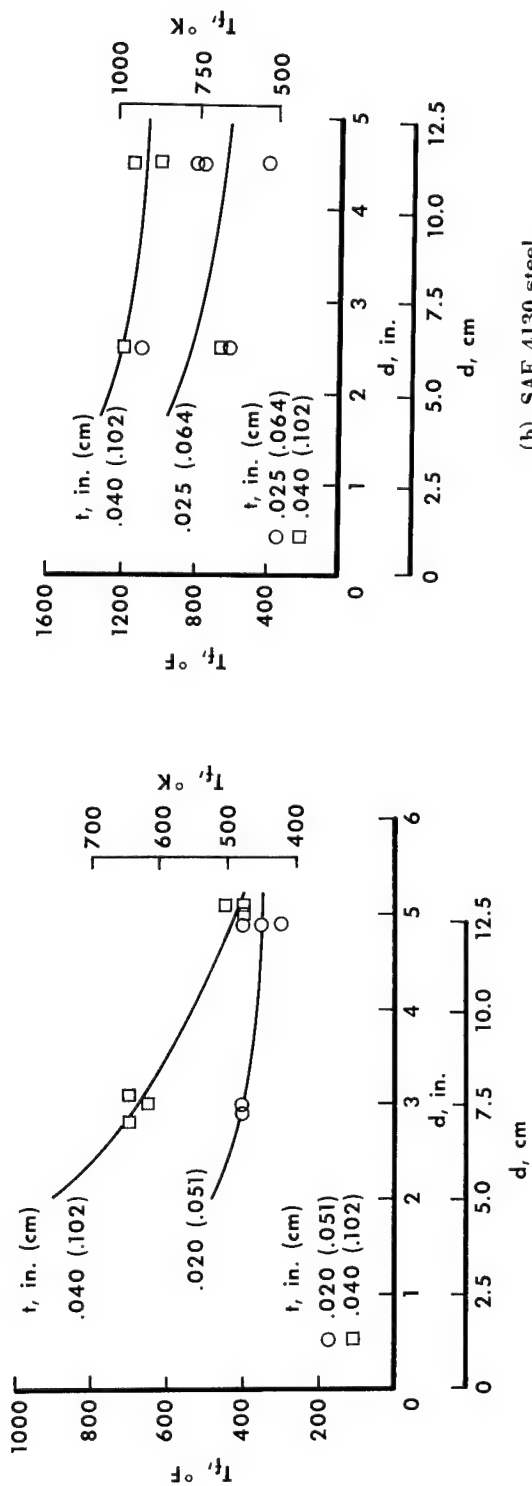
Radius variations had little effect on the failure temperature of the specimens. The failure temperature was affected primarily by flange depth and flange thickness, since the radii and thicknesses investigated were of such proportions that buckling of the cylindrical part of the specimens is an unlikely mode of failure.

INTERPRETATION OF DATA

The buckling characteristics of the specimens are presented in figures 10(a) to 10(c) as a function of the flange depth d and the stagnation-line-failure temperature T_f . Curves representing the specimen thicknesses are faired through the corresponding groups of data. The experimentally determined curves provide the stagnation-line temperatures at which failure occurs for a leading edge with a given flange depth and thickness.

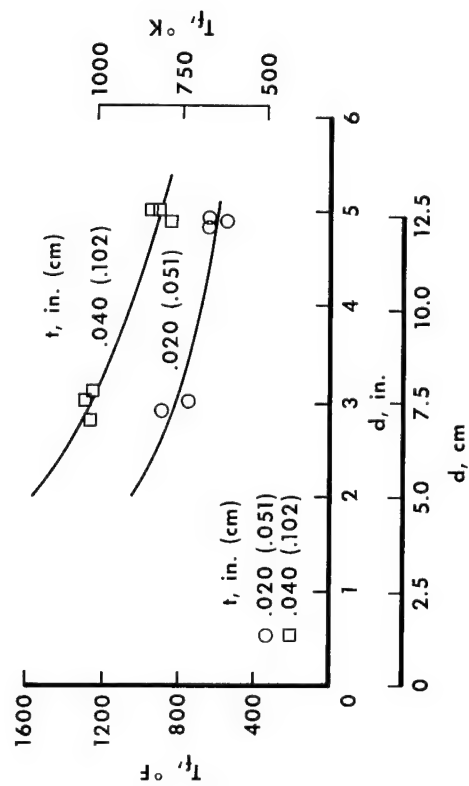
The data plotted in figure 10(a) for the 2024-T3 aluminum specimens are closely grouped; however, the data for the SAE 4130 steel specimens (fig. 10(b)) are somewhat erratic and widely scattered. The point at $d = 2.5$ inches (6.35 cm), $T_f = 600^\circ \text{ F}$ (589° K), and $t = 0.040$ inch (0.102 cm) is considered a "wild" point and was not used in fairing the constant-thickness curves. The data for the Inconel X-750 specimens (fig. 10(c)) are the most closely grouped of the three materials tested.

The general trend of the data presented in figure 10 appears to be logical. The failure temperature increases as the flange depth decreases. A zero flange depth implies an almost semicylindrical shell type of configuration. The cylindrical portions of the specimens were found to have a very high buckling strength, due primarily to their small radii and large shell thicknesses. This characteristic is manifested by the absence of failures in the cylindrical parts of the specimens. Therefore, a rapid increase in failure temperature would be expected as the flange depth approaches zero. It is also logical to expect, for the type of thermal loadings investigated, that, as the flange depth becomes very large, the failure temperature should not be affected and each curve representing constant thickness should approach some constant failure temperature asymptotically. This characteristic is illustrated in figure 10 by the tendency of the faired curves to approach zero slope for the larger flange depths.



(a) 2024-T3 aluminum.

(b) SAE 4130 steel.



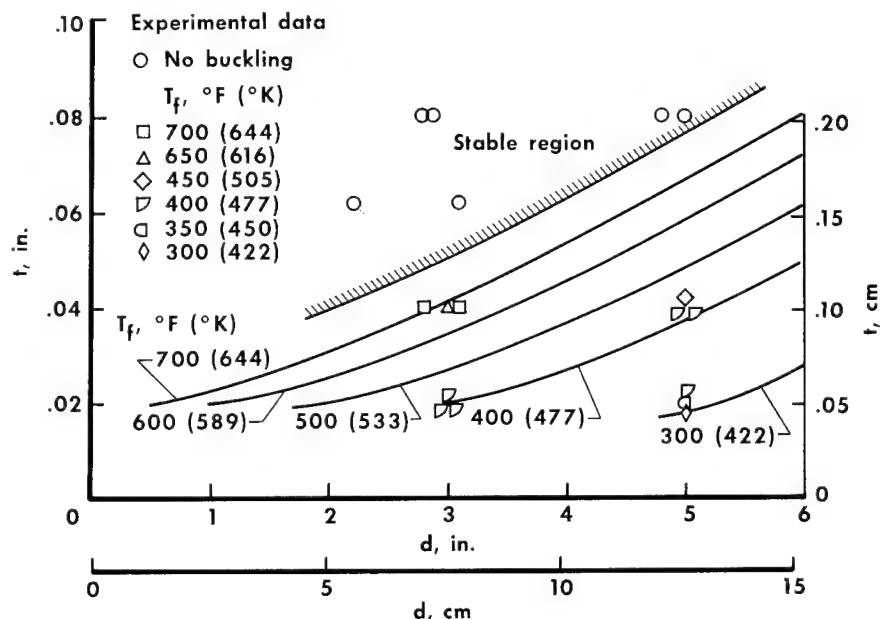
(c) Inconel X-750.

Figure 10.— Variation of the stagnation-line-failure temperatures with the flange depth for two thicknesses.

Figures 11(a), 11(b), and 11(c) illustrate the manner in which the stagnation-line-failure temperature varies for different flange depths and thicknesses. The constant-failure-temperature curves were determined from the data shown in these plots and from the results of figures 10(a), 10(b), and 10(c). A stable region (representing specimens that did not buckle during the experiments) was established by considering the general trends of the curves representing constant failure temperature and the location of the data obtained from the specimens that did not buckle.

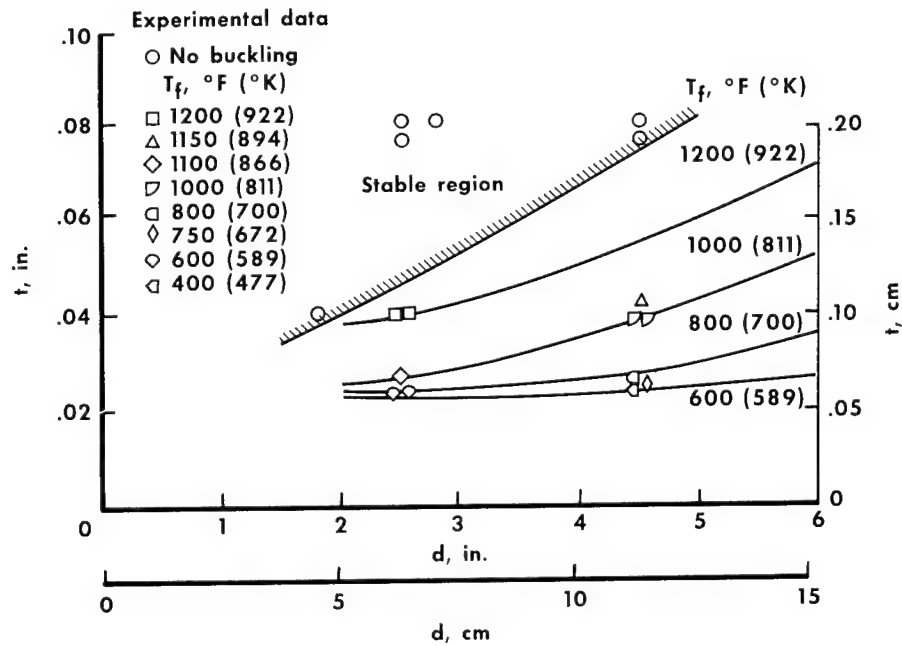
The data in figure 11(a) for the 2024-T3 aluminum specimens are consistent, and the curves representing constant failure temperature were easily established. The data in figure 11(b) for the SAE 4130 steel specimens are somewhat inconsistent, and considerable scatter is apparent. The curves representing constant failure temperature were difficult to establish; however, most of the points were consistent enough to make it possible to locate the curves. The data for the Inconel X-750 specimens in figure 11(c) were consistent, and the curves representing constant failure temperature were easily located.

The results presented in figure 11 demonstrate further the general observations discussed previously. The failure temperature becomes larger for increasing flange thickness and decreasing flange depth. The data for the Inconel X-750 specimens (fig. 11(c)) indicate slightly steeper constant-failure-temperature curves for large failure temperatures. In addition, some of the curves intersect the region in which no buckling occurred (stable region). This illustrates that there are geometric limitations on the failure-temperature curves, which, if exceeded, will exclude buckling as the likely mode of failure for the specific thermal loading applied to the specimen.

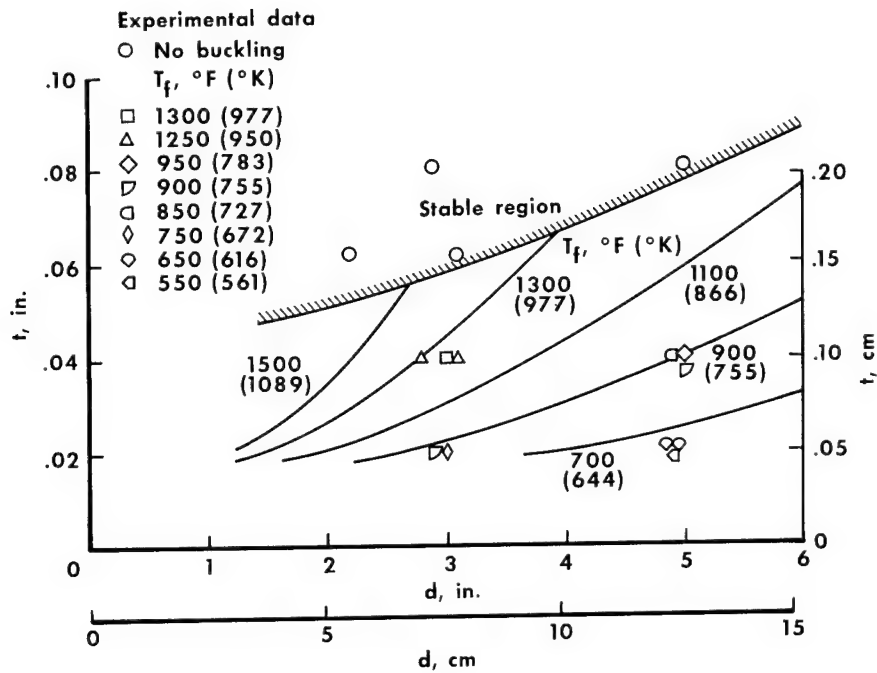


(a) 2024-T3 aluminum.

Figure 11.— Effect of flange depth and flange thickness on the stagnation-line-failure temperature.



(b) SAE 4130 steel.



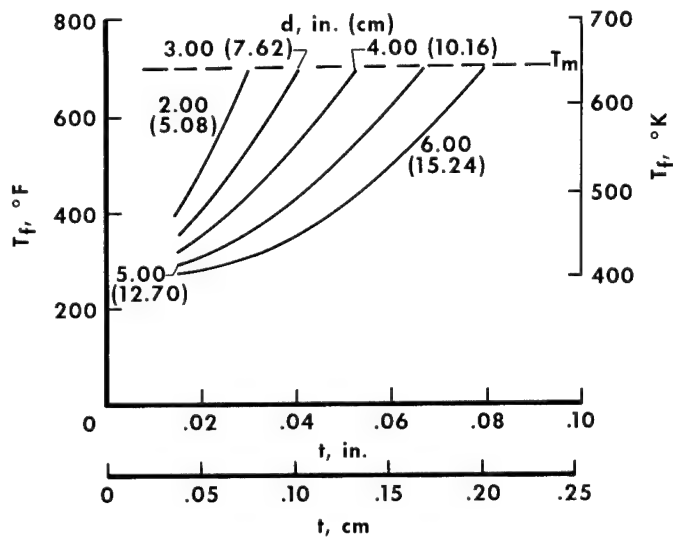
(c) Inconel X-750.

Figure 11.— Concluded.

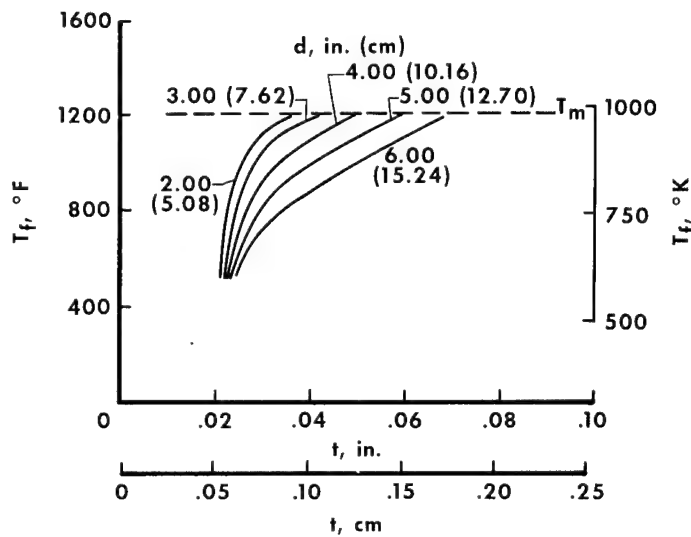
The constant-flange-depth curves shown in figures 12(a), 12(b), and 12(c) were obtained by cross-plotting the information in figures 11(a), 11(b), and 11(c), respectively. The results of such cross-plotting are families of flange-depth curves from which a stagnation-line-failure temperature T_f can be obtained for a specific flange thickness t .

The cross-plots in figures 12(a), 12(b), and 12(c) show that the constant-depth curves converge for small values of flange thickness and, as the flange depths increase, the curves tend to approach a more horizontal position. This trend indicates that, as the flange depth becomes very large, the failure temperature tends to approach a single value for small thicknesses. This observation is conversely coincident with the previous observation that, as the flange depth becomes infinite, each curve representing constant thickness should approach some constant-failure temperature asymptotically. The region in which buckling did not occur is shown in figure 12(c). This region does not appear in figures 12(a) and 12(b), because the curves of constant-failure temperature do not intersect the stable regions in figures 11(a) and 11(b). The dashed lines in figure 12 represent the maximum experimental temperature T_m to which the specimens were subjected. No data were extrapolated beyond this temperature.

The results of the experiment are shown in a different manner in figure 13. A flange parameter $\frac{d}{t}$ is plotted against a buckling parameter $\alpha \Delta T_f \left(\frac{d}{t}\right)^2$ for each of the specimens in which buckling occurred. The introduction of the buckling parameter allows the data to be presented with a parameter describing a physical property of the materials used in the experiment. The coefficient of thermal expansion α is introduced in addition to the

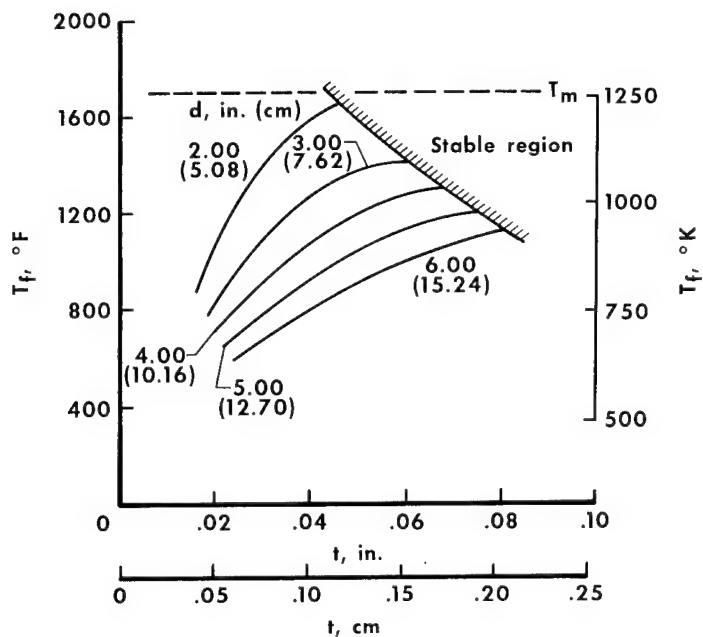


(a) 2024-T3 aluminum.



(b) SAE 4130 steel.

Figure 12.— Variation of stagnation-line-failure temperature as a function of flange thickness for several flange depths.



(c) Inconel X-750.

Figure 12.— Concluded.

temperature change at failure ΔT_f and the flange parameter $\frac{d}{t}$.

Except for a certain amount of scatter, which is characteristic of this type of experiment, the data are fairly closely grouped and appear to be almost linear when presented in terms of these parameters.

The experimental data in figure 13 indicate a consistency between the results obtained for all three materials when the coefficient of thermal expansion and the temperature rise at failure are associated with the geometric parameters. The uniform location of the data leads to the question of whether data obtained for other materials, tested in a similar manner, would

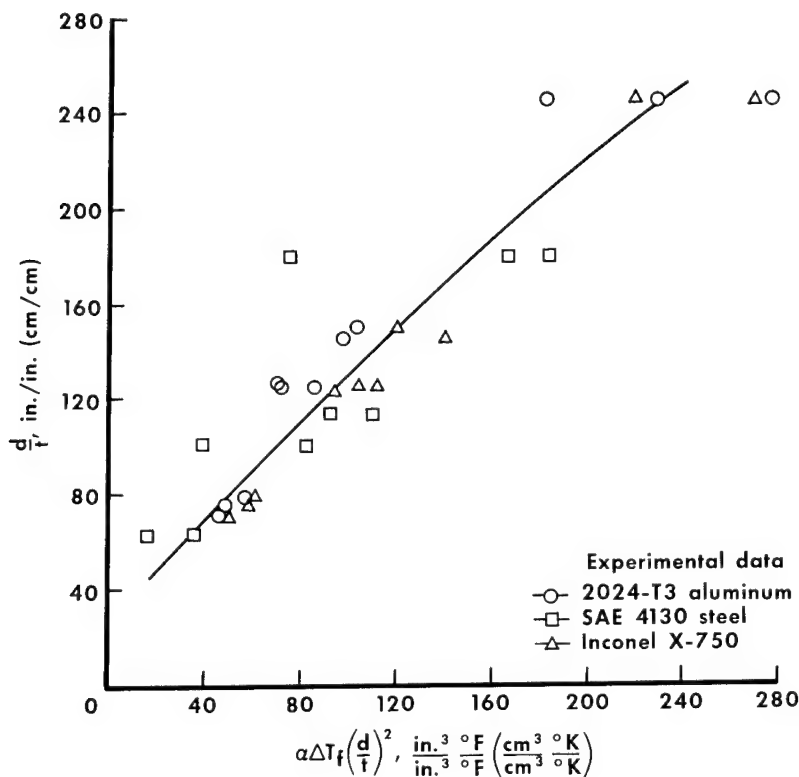


Figure 13.— Effect of the variation of the flange parameter on the buckling parameter.

also lie near the experimental curve obtained in this paper. Although the three materials investigated provide a fairly broad range of physical properties, the range is far from complete. Other materials may behave similarly; however, the scope of these experiments does not warrant any conclusion in this direction.

The faired curve in figure 13 may be closely represented by a parabolic curve of the form

$$x = a_1 + a_2 y + a_3 y^2$$

where

$$x = \alpha \Delta T_f \left(\frac{d}{t} \right)^2$$

$$y = \left(\frac{d}{t} \right)$$

$$a_1, a_2, a_3 = \text{arbitrary constants}$$

The following constants

$$a_1 = -20.72$$

$$a_2 = 0.8013$$

$$a_3 = 0.0009795$$

satisfy the faired curve and yield the equation

$$\alpha \Delta T_f \left(\frac{d}{t} \right)^2 = -20.72 + 0.8013 \left(\frac{d}{t} \right) + 0.0009795 \left(\frac{d}{t} \right)^2$$

Solving for ΔT_f results in the equation

$$\Delta T_f = \frac{1}{\alpha} \left[-20.72 \left(\frac{t}{d} \right)^2 + 0.8013 \left(\frac{t}{d} \right) + 0.0009795 \right]$$

which represents empirically the experimental data of figure 13. The equation may be used to establish the increment of temperature ΔT_f at which leading-edge buckling will occur, if the configuration and the thermal environment are within the experimental limitations of this paper and the material, flange depth, and flange thickness are known. It should again be pointed out that the scope of this paper does not establish the validity of this equation for use with materials other than those included in the experiments.

CONCLUSIONS

Start

An investigation of the buckling behavior of 51 flanged, thin-shell leading-edge specimens subjected to temperature rise rates up to 50° F per sec (27.7° K per sec), which corresponds to a maximum heating rate up to 19.6 Btu/ft²-sec (222.4 kW/m²), showed that:

1. Two modes of buckling occurred in the flanges of most of the specimens. Buckling did not occur in the radial portion of the specimens.

2. The severity of the buckling increased as the thickness of the specimen decreased. The specimen radius affected the failure temperature only slightly.

3. Failure temperatures increased as leading-edge-flange depths decreased, for constant values of thickness. Failure temperatures approached a constant value as the leading-edge-flange depth became large for constant values of thickness.

4. The failure temperature increased as the flange thickness increased for constant values of flange depth.

5. Leading-edge thermal buckling will not occur in particular dimensional regions, provided the maximum stagnation-line temperature is not exceeded, and the leading-edge temperature distribution is similar or less severe than the experimental environment.

6. A unified approach may be implemented to predict thermal buckling of flanged, thin-shell leading edges by associating a property of the leading-edge material (the coefficient of thermal expansion) with the increment of temperature required to initiate buckling and with the geometric parameters of the flange. The experiments led to the following empirical equation

$$\Delta T_f = \frac{1}{\alpha} \left[-20.72 \left(\frac{t}{d} \right)^2 + 0.8013 \left(\frac{t}{d} \right) + 0.0009795 \right]$$

where

for ΔT_f (= incremental rise above room temperature at failure, °F (°K))

α = coefficient of thermal expansion, in./in.°F (cm/cm°K)

t = sheet thickness, in. (cm)

d = flange depth, in. (cm)

To p. 1

Flight Research Center,
National Aeronautics and Space Administration,
Edwards, Calif., October 22, 1965.

REFERENCES

1. Watts, Joe D.; and Banas, Ronald P.: X-15 Structural Temperature Measurements and Calculations for Flights to Maximum Mach Numbers of Approximately 4, 5, and 6. NASA TM X-883, 1963.
2. Kordes, Eldon E.; Reed, Robert D.; and Dawdy, Alpha L.: Structural Heating Experiences on the X-15 Airplane. NASA TM X-711, 1962.
3. Anthony, Frank M.; Merrihew, Fred A.; Mistretta, Andrew L.; and Dukes, Wilfred H.: Investigation of Feasibility of Utilizing Available Heat-Resistant Materials for Hypersonic Leading Edge Applications. Vol. I - Summary. WADC Tech. Rep. 59-744, U.S. Air Force, Jan. 1961.
4. Anthony, F. M.; Blessing, A. H.; Buckley, W. H.; and Dukes, W. H.: Investigation of Feasibility of Utilizing Available Heat Resistant Materials for Hypersonic Leading Edge Applications. Vol. II - Analytical Methods and Design Studies. WADC Tech. Rep. 59-744, U.S. Air Force, March 1961. (Available from ASTIA as AD 265 083.)
5. Mansfield, E. H.: Leading-Edge Buckling Due to Aerodynamic Heating. R. & M. No. 3197, British A.R.C., 1960.
6. McKenzie, K. I.: The Leading-Edge Buckling of a Thin Built-Up Wing Due to Aerodynamic Heating. R. & M. No. 3295, British A.R.C., 1962.
7. Mechtly, E. A.: The International System of Units - Physical Constants and Conversion Factors. NASA SP-7012, 1964.
8. Anon.: Aerospace Structural Metals Handbook. Vol. II - Non-Ferrous Alloys. Syracuse Univ. Press (Box 87 University Station, Syracuse, New York), Mar. 1963.
9. Morozov, E. M.; and Fridman, Ya. B.: Thermal Stresses and Their Calculation. Strength and Deformation in Nonuniform Temperature Fields, Prof. Ya. B. Fridman, ed., Consultants Bureau (227 W. 17th St., New York), 1964, pp. 17-61. (Transl. from the Russian.)

TABLE I
GEOMETRY OF LEADING-EDGE SPECIMENS

| Specimen | Material | r, in. (cm) | d, in. (cm) | t, in. (cm) | r/t | d/t |
|----------|------------------|-------------|--------------|--------------|------|-----|
| 1 | 2024-T3 Aluminum | 0.50 (1.27) | 2.90 (7.37) | 0.080 (.203) | 6.3 | 36 |
| 2 | 2024-T3 Aluminum | .50 (1.27) | 5.00 (12.70) | .080 (.203) | 6.3 | 63 |
| 3 | 2024-T3 Aluminum | .25 (.64) | 2.80 (7.11) | .080 (.203) | 3.1 | 35 |
| 4 | 2024-T3 Aluminum | .25 (.64) | 4.80 (12.19) | .080 (.203) | 3.1 | 60 |
| 5 | 2024-T3 Aluminum | .50 (1.27) | 3.00 (7.62) | .040 (.102) | 12.5 | 75 |
| 6 | 2024-T3 Aluminum | .50 (1.27) | 5.00 (12.70) | .040 (.102) | 12.5 | 125 |
| 7 | 2024-T3 Aluminum | 1.00 (2.54) | 5.00 (12.70) | .040 (.102) | 25.0 | 125 |
| 8 | 2024-T3 Aluminum | 1.00 (2.54) | 3.10 (7.62) | .040 (.102) | 25.0 | 78 |
| 9 | 2024-T3 Aluminum | 1.00 (2.54) | 4.90 (12.45) | .020 (.051) | 50.0 | 245 |
| 10 | 2024-T3 Aluminum | 1.00 (2.54) | 3.00 (7.62) | .020 (.051) | 50.0 | 150 |
| 11 | 2024-T3 Aluminum | .50 (1.27) | 4.90 (12.45) | .020 (.051) | 25.0 | 245 |
| 12 | 2024-T3 Aluminum | .50 (1.27) | 3.00 (7.62) | .020 (.051) | 25.0 | 150 |
| 13 | 2024-T3 Aluminum | .25 (.64) | 4.90 (12.45) | .040 (.102) | 6.3 | 123 |
| 14 | 2024-T3 Aluminum | .25 (.64) | 2.80 (7.11) | .040 (.102) | 6.3 | 70 |
| 15 | 2024-T3 Aluminum | .25 (.64) | 4.90 (12.45) | .020 (.051) | 12.5 | 245 |
| 16 | 2024-T3 Aluminum | .25 (.64) | 2.90 (7.37) | .020 (.051) | 12.5 | 145 |
| 17 | 2024-T3 Aluminum | .88 (2.22) | 2.20 (5.59) | .063 (.160) | 13.9 | 35 |
| 18 | 2024-T3 Aluminum | .88 (2.22) | 3.10 (7.62) | .063 (.160) | 13.9 | 49 |
| 19 | SAE 4130 Steel | .50 (1.27) | 2.50 (6.35) | .080 (.203) | 6.3 | 31 |
| 20 | SAE 4130 Steel | .50 (1.27) | 4.50 (11.43) | .080 (.203) | 6.3 | 56 |
| 21 | SAE 4130 Steel | .25 (.64) | 2.50 (6.35) | .080 (.203) | 3.1 | 31 |
| 22 | SAE 4130 Steel | .25 (.64) | 4.50 (11.43) | .080 (.203) | 3.1 | 56 |
| 23 | SAE 4130 Steel | .50 (1.27) | 2.50 (6.35) | .040 (.102) | 12.5 | 63 |
| 24 | SAE 4130 Steel | .50 (1.27) | 4.50 (11.43) | .040 (.102) | 12.5 | 113 |
| 25 | SAE 4130 Steel | 1.00 (2.54) | 4.50 (11.43) | .040 (.102) | 25.0 | 113 |
| 26 | SAE 4130 Steel | 1.00 (2.54) | 2.50 (6.35) | .040 (.102) | 25.0 | 63 |
| 27 | SAE 4130 Steel | 1.00 (2.54) | 4.50 (11.43) | .025 (.064) | 40.0 | 180 |
| 28 | SAE 4130 Steel | 1.00 (2.54) | 2.50 (6.35) | .025 (.064) | 40.0 | 100 |
| 29 | SAE 4130 Steel | .50 (1.27) | 4.50 (11.43) | .025 (.064) | 20.0 | 180 |
| 30 | SAE 4130 Steel | .50 (1.27) | 2.50 (6.35) | .025 (.064) | 20.0 | 100 |
| 31 | SAE 4130 Steel | .25 (.64) | 4.50 (11.43) | .040 (.102) | 6.3 | 113 |
| 32 | SAE 4130 Steel | .25 (.64) | 2.50 (6.35) | .040 (.102) | 6.3 | 63 |
| 33 | SAE 4130 Steel | .25 (.64) | 4.50 (11.43) | .025 (.064) | 10.0 | 180 |
| 34 | SAE 4130 Steel | .25 (.64) | 2.50 (6.35) | .025 (.064) | 10.0 | 100 |
| 35 | SAE 4130 Steel | 1.00 (2.54) | 2.80 (7.11) | .080 (.203) | 12.5 | 35 |
| 36 | SAE 4130 Steel | 1.00 (2.54) | 1.80 (4.57) | .040 (.102) | 25.0 | 45 |
| 37 | Inconel X-750 | .50 (1.27) | 2.90 (7.37) | .078 (.198) | 6.4 | 37 |
| 38 | Inconel X-750 | .50 (1.27) | 5.00 (12.70) | .078 (.198) | 6.4 | 64 |
| 39 | Inconel X-750 | .50 (1.27) | 3.00 (7.62) | .040 (.102) | 12.5 | 75 |
| 40 | Inconel X-750 | .50 (1.27) | 5.00 (12.70) | .040 (.102) | 12.5 | 125 |
| 41 | Inconel X-750 | 1.00 (2.54) | 5.00 (12.70) | .040 (.102) | 25.0 | 125 |
| 42 | Inconel X-750 | 1.00 (2.54) | 3.10 (7.62) | .040 (.102) | 25.0 | 78 |
| 43 | Inconel X-750 | 1.00 (2.54) | 4.90 (12.45) | .020 (.051) | 50.0 | 245 |
| 44 | Inconel X-750 | 1.00 (2.54) | 3.00 (7.62) | .020 (.051) | 50.0 | 150 |
| 45 | Inconel X-750 | .50 (1.27) | 4.90 (12.45) | .020 (.051) | 25.0 | 245 |
| 46 | Inconel X-750 | .25 (.64) | 4.90 (12.45) | .040 (.102) | 6.3 | 123 |
| 47 | Inconel X-750 | .25 (.64) | 2.80 (7.11) | .040 (.102) | 6.3 | 70 |
| 48 | Inconel X-750 | .25 (.64) | 4.90 (12.45) | .020 (.051) | 12.5 | 245 |
| 49 | Inconel X-750 | .25 (.64) | 2.90 (7.37) | .020 (.051) | 12.5 | 145 |
| 50 | Inconel X-750 | .88 (2.22) | 2.20 (5.59) | .062 (.157) | 14.1 | 35 |
| 51 | Inconel X-750 | .88 (2.22) | 3.10 (7.62) | .062 (.157) | 14.1 | 50 |

TABLE II

DESCRIPTION OF LEADING-EDGE-SPECIMEN THERMOCOUPLE LOCATIONS

| Specimen | a, in. (cm) | b, in. (cm) | c, in. (cm) |
|----------|-------------|-------------|-------------|
| 1 | 0.38 (0.97) | 1.50 (3.81) | 2.50 (6.35) |
| 2 | .38 (.97) | 1.50 (3.81) | 2.50 (6.35) |
| 3 | .38 (.97) | 1.50 (3.81) | 2.50 (6.35) |
| 4 | .38 (.97) | 1.50 (3.81) | 2.50 (6.35) |
| 5 | .38 (.97) | 1.50 (3.81) | 2.50 (6.35) |
| 6 | .38 (.97) | 1.50 (3.81) | 2.50 (6.35) |
| 7 | .38 (.97) | 1.50 (3.81) | 2.50 (6.35) |
| 8 | .38 (.97) | 1.50 (3.81) | 2.50 (6.35) |
| 9 | .38 (.97) | 1.50 (3.81) | 2.50 (6.35) |
| 10 | .38 (.97) | 1.50 (3.81) | 2.50 (6.35) |
| 11 | .38 (.97) | 1.50 (3.81) | 2.50 (6.35) |
| 12 | .38 (.97) | 1.50 (3.81) | 2.50 (6.35) |
| 13 | .38 (.97) | 1.50 (3.81) | 2.50 (6.35) |
| 14 | .38 (.97) | 1.50 (3.81) | 2.50 (6.35) |
| 15 | .38 (.97) | 1.50 (3.81) | 2.50 (6.35) |
| 16 | .38 (.97) | 1.50 (3.81) | 2.50 (6.35) |
| 17 | .38 (.97) | 1.50 (3.81) | 2.50 (6.35) |
| 18 | .38 (.97) | 1.50 (3.81) | 2.50 (6.35) |
| 19 | .38 (.97) | 1.00 (2.54) | 2.00 (5.08) |
| 20 | .38 (.97) | 1.50 (3.81) | 2.50 (6.35) |
| 21 | .38 (.97) | 1.00 (2.54) | 2.00 (5.08) |
| 22 | .38 (.97) | 1.50 (3.81) | 2.50 (6.35) |
| 23 | .38 (.97) | 1.00 (2.54) | 2.00 (5.08) |
| 24 | .38 (.97) | 1.50 (3.81) | 2.50 (6.35) |
| 25 | .38 (.97) | 1.50 (3.81) | 2.50 (6.35) |
| 26 | .38 (.97) | 1.00 (2.54) | 2.00 (5.08) |
| 27 | .38 (.97) | 1.50 (3.81) | 2.50 (6.35) |
| 28 | .38 (.97) | 1.00 (2.54) | 2.00 (5.08) |
| 29 | .38 (.97) | 1.50 (3.81) | 2.50 (6.35) |
| 30 | .38 (.97) | 1.00 (2.54) | 2.00 (5.08) |
| 31 | .38 (.97) | 1.50 (3.81) | 2.50 (6.35) |
| 32 | .38 (.97) | 1.00 (2.54) | 2.00 (5.08) |
| 33 | .38 (.97) | 1.50 (3.81) | 2.50 (6.35) |
| 34 | .38 (.97) | 1.00 (2.54) | 2.00 (5.08) |
| 35 | .38 (.97) | 1.00 (2.54) | 2.00 (5.08) |
| 36 | .38 (.97) | 1.00 (2.54) | 2.00 (5.08) |
| 37 | .38 (.97) | 1.00 (2.54) | 2.00 (5.08) |
| 38 | .38 (.97) | 1.50 (3.81) | 2.50 (6.35) |
| 39 | .38 (.97) | 1.00 (2.54) | 2.00 (5.08) |
| 40 | .38 (.97) | 1.50 (3.81) | 2.50 (6.35) |
| 41 | .38 (.97) | 1.50 (3.81) | 2.50 (6.35) |
| 42 | .38 (.97) | 1.50 (3.81) | 2.50 (6.35) |
| 43 | .38 (.97) | 1.50 (3.81) | 2.50 (6.35) |
| 44 | .38 (.97) | 1.50 (3.81) | 2.50 (6.35) |
| 45 | .38 (.97) | 1.50 (3.81) | 2.50 (6.35) |
| 46 | .38 (.97) | 1.00 (2.54) | 2.00 (5.08) |
| 47 | .38 (.97) | 1.50 (3.81) | 2.50 (6.35) |
| 48 | .38 (.97) | 1.50 (3.81) | 2.50 (6.35) |
| 49 | .38 (.97) | 1.00 (2.54) | 2.00 (5.08) |
| 50 | .38 (.97) | 1.00 (2.54) | 2.00 (5.08) |
| 51 | .38 (.97) | 1.50 (3.81) | 2.50 (6.35) |

TABLE III
SUMMARY OF RESULTS OF LEADING-EDGE EXPERIMENTS

| Specimen number | Unstable behavior | | | | Stable behavior |
|-----------------|---------------------|---|---------------------|---|--|
| | Mode 1 | | Mode 2 | | |
| | Severity of failure | Stagnation-line temperature at failure, °F (°K) | Severity of failure | Stagnation-line temperature at failure, °F (°K) | Maximum temperature attained by stable specimen, °F (°K) |
| 1 | None | ----- | None | ----- | 690 (638) |
| 2 | None | ----- | None | ----- | 700 (644) |
| 3 | None | ----- | None | ----- | 710 (649) |
| 4 | None | ----- | None | ----- | 700 (644) |
| 5 | None | ----- | Moderate | 650 (620) | ----- |
| 6 | Moderate | ^a 700 (644) | Moderate | 450 (505) | ----- |
| 7 | None | ----- | Severe | 400 (477) | ----- |
| 8 | None | ----- | Severe | 700 (674) | ----- |
| 9 | None | ----- | Severe | 350 (450) | ----- |
| 10 | Moderate | 500 (533) | Severe | 400 (477) | ----- |
| 11 | Moderate | 500 (533) | Severe | 400 (477) | ----- |
| 12 | Severe | 400 (477) | Severe | 400 (477) | ----- |
| 13 | Moderate | 400 (477) | Severe | 400 (477) | ----- |
| 14 | Severe | 700 (644) | None | ----- | ----- |
| 15 | Severe | 700 (644) | Severe | 300 (422) | ----- |
| 16 | Gross | 400 (477) | Gross | 400 (477) | ----- |
| 17 | None | ----- | None | ----- | 710 (649) |
| 18 | None | ----- | None | ----- | 700 (644) |
| 19 | None | ----- | None | ----- | 1170 (905) |
| 20 | None | ----- | None | ----- | 1160 (900) |
| 21 | None | ----- | None | ----- | 1140 (888) |
| 22 | None | ----- | None | ----- | 1170 (905) |
| 23 | Moderate | ^a 1200 (922) | None | ----- | ----- |
| 24 | Moderate | 1150 (894) | Moderate | 1150 (894) | ----- |
| 25 | Moderate | 1000 (811) | Gross | 1000 (811) | ----- |
| 26 | None | ----- | Gross | 600 (589) | ----- |
| 27 | None | ----- | Gross | 800 (700) | ----- |
| 28 | None | ----- | Gross | 1100 (866) | ----- |
| 29 | Moderate | 750 (663) | Gross | 750 (663) | ----- |
| 30 | Moderate | 700 (644) | Gross | 600 (589) | ----- |
| 31 | Severe | 1000 (811) | Moderate | 1000 (811) | ----- |
| 32 | Severe | 1200 (922) | None | ----- | ----- |
| 33 | Severe | 1000 (811) | Gross | 400 (477) | ----- |
| 34 | Gross | 600 (589) | Gross | 600 (589) | ----- |
| 35 | None | ----- | None | ----- | 1220 (933) |
| 36 | None | ----- | None | ----- | 1190 (916) |
| 37 | None | ----- | None | ----- | 1690 (1194) |
| 38 | None | ----- | None | ----- | 1720 (1211) |
| 39 | None | ----- | Moderate | 1300 (977) | ----- |
| 40 | Moderate | 1100 (866) | Severe | 950 (783) | ----- |
| 41 | None | ----- | Severe | 900 (755) | ----- |
| 42 | None | ----- | Severe | 1250 (950) | ----- |
| 43 | Moderate | 600 (589) | Severe | 550 (561) | ----- |
| 44 | Moderate | 800 (700) | Severe | 750 (633) | ----- |
| 45 | Severe | 800 (700) | Severe | 650 (616) | ----- |
| 46 | Severe | 900 (755) | Severe | 850 (727) | ----- |
| 47 | Moderate | 1250 (950) | Severe | 1250 (950) | ----- |
| 48 | ^b Gross | 650 (616) | ^b Gross | 650 (616) | ----- |
| 49 | ^b Gross | 900 (755) | ^b Gross | 900 (755) | ----- |
| 50 | None | ----- | None | ----- | 1760 (1233) |
| 51 | None | ----- | None | ----- | 1700 (1199) |

^aSpecimen buckled during 10-second heat soak at maximum temperature.

^bSpecimen cracked.

TABLE IV

CHORDWISE TEMPERATURE-TIME HISTORIES OF THE SPECIMENS

| Specimen number | Time, sec | Temperature, °F (°K) | | | |
|-----------------|-----------|----------------------|----------------|----------------|----------------|
| | | Thermocouple 2 | Thermocouple 3 | Thermocouple 4 | Thermocouple 5 |
| 1 | 0 | 80 (300) | 80 (300) | 80 (300) | 80 (300) |
| 1 | 5 | 220 (377) | 200 (366) | 100 (311) | 80 (300) |
| 1 | 10 | 430 (494) | 360 (455) | 120 (322) | 100 (311) |
| 1 | 15 | 610 (594) | 500 (533) | 200 (366) | 120 (322) |
| 1 | 20 | 690 (639) | 550 (561) | 270 (405) | 180 (355) |
| 1 | 25 | 650 (616) | 560 (566) | 330 (430) | 200 (366) |
| 2 | 0 | 80 (300) | 80 (300) | 80 (300) | 80 (300) |
| 2 | 5 | 340 (444) | 160 (344) | 90 (305) | 90 (305) |
| 2 | 10 | 600 (588) | 300 (422) | 120 (322) | 100 (311) |
| 2 | 15 | 700 (644) | 440 (500) | 200 (366) | 120 (322) |
| 2 | 20 | 700 (644) | 500 (533) | 260 (400) | 160 (344) |
| 2 | 25 | 640 (611) | 520 (544) | 300 (422) | 180 (355) |
| 3 | 0 | 80 (300) | 80 (300) | 80 (300) | 80 (300) |
| 3 | 5 | 370 (461) | 280 (411) | 80 (300) | 80 (300) |
| 3 | 10 | 620 (600) | 440 (600) | 140 (333) | 100 (311) |
| 3 | 15 | 700 (644) | 600 (588) | 220 (370) | 120 (322) |
| 3 | 20 | 700 (644) | 620 (600) | 270 (405) | 160 (344) |
| 3 | 25 | 640 (611) | 600 (588) | 300 (422) | 180 (355) |
| 4 | 0 | 80 (300) | 80 (300) | 80 (300) | 80 (300) |
| 4 | 5 | 370 (461) | 300 (422) | 120 (322) | 100 (311) |
| 4 | 10 | 630 (605) | 520 (544) | 210 (373) | 120 (322) |
| 4 | 15 | 700 (644) | 620 (600) | 300 (422) | 180 (355) |
| 4 | 20 | 700 (644) | 640 (611) | 370 (461) | 220 (377) |
| 4 | 25 | 640 (611) | 600 (588) | 400 (477) | 240 (389) |
| 5 | 0 | 80 (300) | 80 (300) | 80 (300) | 80 (300) |
| 5 | 5 | 400 (477) | 240 (389) | 100 (310) | 100 (311) |
| 5 | 10 | 640 (611) | 450 (508) | 140 (333) | 130 (327) |
| 5 | 15 | 700 (644) | 560 (566) | 200 (366) | 160 (344) |
| 5 | 20 | 700 (644) | 600 (588) | 300 (422) | 170 (350) |
| 5 | 25 | 640 (611) | 560 (566) | 350 (450) | 200 (366) |
| 6 | 0 | 80 (300) | 80 (300) | 80 (300) | 80 (300) |
| 6 | 5 | 360 (455) | 220 (377) | 120 (322) | 80 (300) |
| 6 | 10 | 620 (600) | 400 (477) | 190 (361) | 90 (305) |
| 6 | 15 | 700 (644) | 530 (550) | 260 (400) | 110 (316) |
| 6 | 20 | 700 (644) | 570 (572) | 320 (433) | 160 (344) |
| 6 | 25 | 620 (605) | 540 (555) | 350 (450) | 200 (366) |
| 7 | 0 | 80 (300) | 80 (300) | 80 (300) | 80 (300) |
| 7 | 5 | 200 (366) | 140 (333) | 100 (311) | 80 (300) |
| 7 | 10 | 420 (489) | 290 (416) | 160 (344) | 90 (305) |
| 7 | 15 | 660 (622) | 440 (500) | 220 (377) | 120 (322) |
| 7 | 20 | 690 (639) | 520 (544) | 280 (411) | 160 (344) |
| 7 | 25 | 700 (644) | 560 (566) | 340 (444) | 220 (377) |
| 8 | 0 | 80 (300) | 80 (300) | 80 (300) | 80 (300) |
| 8 | 5 | 350 (450) | 180 (355) | 100 (311) | 90 (305) |
| 8 | 10 | 600 (588) | 340 (444) | 160 (344) | 120 (322) |
| 8 | 15 | 700 (644) | 520 (544) | 260 (400) | 160 (344) |
| 8 | 20 | 700 (644) | 580 (577) | 320 (433) | 200 (366) |
| 8 | 25 | 640 (611) | 580 (577) | 360 (455) | 230 (383) |

TABLE IV.- Continued

CHORDWISE TEMPERATURE-TIME HISTORIES OF THE SPECIMENS

| Specimen number | Time, sec | Temperature, °F (°K) | | | |
|--------------------|--------------|----------------------|----------------|----------------|----------------|
| | | Thermocouple 2 | Thermocouple 3 | Thermocouple 4 | Thermocouple 5 |
| 9 | 0 | 80 (300) | 80 (300) | 80 (300) | 80 (300) |
| 9 | 5 | 240 (389) | 160 (344) | 100 (311) | 80 (300) |
| 9 | 10 | 520 (544) | 340 (444) | 160 (344) | 90 (305) |
| 9 | 15 | 720 (655) | 480 (522) | 240 (389) | 110 (316) |
| 9 | 20 | 720 (655) | 540 (555) | 300 (415) | 150 (339) |
| 9 | 25 | 700 (644) | 550 (561) | 340 (444) | 200 (366) |
| 10 | 0 | 80 (300) | 80 (300) | 80 (300) | 80 (300) |
| 10 | 5 | 350 (450) | 270 (405) | 80 (300) | 80 (300) |
| 10 | 10 | 630 (605) | 440 (500) | 130 (327) | 90 (305) |
| 10 | 15 | 710 (649) | 540 (555) | 220 (377) | 120 (322) |
| 10 | 20 | 710 (649) | 580 (577) | 300 (415) | 170 (350) |
| 10 | 25 | 690 (638) | 570 (572) | 320 (433) | 190 (361) |
| 11 | 0 | 80 (300) | 80 (300) | 80 (300) | 80 (300) |
| 11 | 5 | 350 (450) | 230 (383) | 120 (322) | 80 (300) |
| 11 | 10 | 600 (588) | 420 (489) | 200 (366) | 120 (322) |
| 11 | 15 | 710 (650) | 580 (577) | 300 (415) | 160 (344) |
| 11 | 20 | 710 (650) | 600 (588) | 380 (466) | 210 (372) |
| 11 | 25 | 650 (639) | 600 (588) | 400 (477) | 250 (394) |
| 12 | 0 | 80 (300) | 80 (300) | 80 (300) | 80 (300) |
| 12 | 5 | 400 (477) | 290 (416) | 120 (322) | 80 (300) |
| 12 | 10 | 660 (622) | 500 (533) | 230 (383) | 100 (311) |
| 12 | 15 | 720 (655) | 600 (588) | 330 (439) | 140 (333) |
| 12 | 20 | 720 (655) | 600 (588) | 380 (466) | 180 (355) |
| 12 | 25 | 620 (600) | 560 (566) | 380 (466) | 200 (366) |
| 13 | 0 | 80 (300) | 80 (300) | 80 (300) | 80 (300) |
| 13 | 5 | 320 (433) | 240 (389) | 120 (322) | 80 (300) |
| 13 | 10 | 580 (577) | 450 (505) | 220 (377) | 100 (311) |
| 13 | 15 | 700 (644) | 590 (583) | 320 (433) | 150 (339) |
| 13 | 20 | 700 (644) | 600 (588) | 370 (461) | 200 (366) |
| 13 | 25 | 630 (605) | 570 (572) | 390 (472) | 240 (389) |
| 14 | 0 | 80 (300) | 80 (300) | 80 (300) | 80 (300) |
| 14 | 5 | 350 (450) | 260 (400) | 220 (366) | 90 (305) |
| 14 | 10 | 600 (588) | 440 (500) | 390 (472) | 130 (327) |
| 14 | 15 | 700 (644) | 580 (577) | 470 (516) | 200 (366) |
| 14 | 20 | 700 (644) | 600 (589) | 500 (533) | 260 (400) |
| 14 | 25 | 660 (622) | 570 (572) | 490 (527) | 280 (411) |
| 15 | 0 | 80 (300) | 80 (300) | 80 (300) | 80 (300) |
| 15 | 5 | 250 (394) | 160 (344) | 100 (311) | 80 (300) |
| 15 | 10 | 500 (533) | 360 (455) | 180 (355) | 90 (305) |
| 15 | 15 | 700 (644) | 560 (566) | 300 (422) | 120 (322) |
| 15 | 20 | 700 (644) | 600 (589) | 370 (461) | 180 (355) |
| 15 | 25 | 680 (633) | 600 (589) | 400 (477) | 220 (377) |
| 16 | 0 | 80 (300) | 80 (300) | 80 (300) | 80 (300) |
| 16 | 5 | 360 (455) | 250 (394) | 130 (327) | 80 (300) |
| 16 | 10 | 640 (611) | 480 (522) | 220 (377) | 90 (305) |
| 16 | 15 | 720 (655) | 620 (600) | 320 (433) | 120 (322) |
| 16 | 20 | 720 (655) | 640 (611) | 380 (466) | 150 (339) |
| 16 | 25 | 680 (633) | 620 (600) | 400 (477) | 180 (355) |

TABLE IV.- Continued

CHORDWISE TEMPERATURE-TIME HISTORIES OF THE SPECIMENS

| Specimen number | Time, sec | Temperature, °F (°K) | | | |
|-----------------|-----------|----------------------|----------------|----------------|----------------|
| | | Thermocouple 2 | Thermocouple 3 | Thermocouple 4 | Thermocouple 5 |
| 17 | 0 | 80 (300) | 80 (300) | 80 (300) | 80 (300) |
| 17 | 5 | 340 (444) | 130 (327) | 90 (305) | 80 (300) |
| 17 | 10 | 600 (588) | 280 (411) | 120 (322) | 90 (305) |
| 17 | 15 | 690 (639) | 460 (511) | 200 (366) | 110 (316) |
| 17 | 20 | 700 (644) | 530 (550) | 280 (411) | 140 (333) |
| 17 | 25 | 650 (616) | 560 (566) | 330 (439) | 160 (344) |
| 18 | 0 | 80 (300) | 80 (300) | 80 (300) | 80 (300) |
| 18 | 5 | 310 (427) | 230 (383) | 120 (322) | 90 (305) |
| 18 | 10 | 580 (577) | 400 (477) | 200 (366) | 100 (311) |
| 18 | 15 | 700 (644) | 500 (533) | 270 (405) | 130 (327) |
| 18 | 20 | 700 (644) | 560 (566) | 320 (433) | 160 (344) |
| 18 | 25 | 660 (622) | 560 (566) | 360 (455) | 200 (366) |
| 19 | 0 | 80 (300) | 80 (300) | 80 (300) | 80 (300) |
| 19 | 5 | 320 (433) | 180 (355) | 80 (300) | 80 (300) |
| 19 | 10 | 560 (566) | 340 (444) | 90 (305) | 80 (300) |
| 19 | 15 | 790 (694) | 500 (533) | 110 (316) | 80 (300) |
| 19 | 20 | 980 (800) | 640 (611) | 140 (333) | 90 (305) |
| 19 | 25 | 1140 (889) | 760 (677) | 190 (361) | 100 (311) |
| 19 | 30 | 1170 (905) | 800 (700) | 240 (389) | 120 (322) |
| 19 | 35 | 1120 (877) | 820 (711) | 280 (411) | 140 (333) |
| 20 | 0 | 80 (300) | 80 (300) | 80 (300) | 80 (300) |
| 20 | 5 | 330 (439) | 90 (305) | 80 (300) | 80 (300) |
| 20 | 10 | 570 (572) | 140 (333) | 90 (305) | 80 (300) |
| 20 | 15 | 800 (700) | 220 (377) | 100 (311) | 80 (300) |
| 20 | 20 | 1000 (811) | 300 (415) | 130 (327) | 80 (300) |
| 20 | 25 | 1150 (894) | 400 (477) | 170 (350) | 80 (300) |
| 20 | 30 | 1150 (894) | 460 (511) | 210 (372) | 90 (305) |
| 20 | 35 | 1100 (866) | 500 (533) | 250 (394) | 100 (311) |
| 21 | 0 | 80 (300) | 80 (300) | 80 (300) | 80 (300) |
| 21 | 5 | 330 (439) | 200 (366) | 80 (300) | 80 (300) |
| 21 | 10 | 590 (583) | 340 (444) | 120 (322) | 80 (300) |
| 21 | 15 | 770 (683) | 500 (533) | 180 (355) | 90 (305) |
| 21 | 20 | 950 (788) | 640 (611) | 240 (389) | 100 (311) |
| 21 | 25 | 1100 (866) | 760 (677) | 300 (415) | 130 (327) |
| 21 | 30 | 1120 (877) | 820 (711) | 350 (450) | 150 (339) |
| 21 | 35 | 1040 (833) | 820 (711) | 400 (477) | 180 (355) |
| 22 | 0 | 80 (300) | 80 (300) | 80 (300) | 80 (300) |
| 22 | 5 | 350 (450) | 200 (366) | 80 (300) | 80 (300) |
| 22 | 10 | 600 (588) | 380 (466) | 100 (311) | 80 (300) |
| 22 | 15 | 830 (716) | 550 (581) | 130 (327) | 80 (300) |
| 22 | 20 | 1020 (822) | 700 (644) | 170 (350) | 90 (305) |
| 22 | 25 | 1180 (911) | 850 (727) | 220 (377) | 100 (311) |
| 22 | 30 | 1170 (905) | 880 (744) | 260 (400) | 110 (316) |
| 22 | 35 | 1040 (833) | 840 (722) | 290 (416) | 120 (322) |

TABLE IV.- Continued

CHORDWISE TEMPERATURE-TIME HISTORIES OF THE SPECIMENS

| Specimen number | Time, sec | Temperature, °F (°K) | | | |
|-----------------|-----------|----------------------|----------------|----------------|----------------|
| | | Thermocouple 2 | Thermocouple 3 | Thermocouple 4 | Thermocouple 5 |
| 23 | 0 | 80 (300) | 80 (300) | 80 (300) | 80 (300) |
| 23 | 5 | 320 (433) | 220 (377) | 90 (305) | 80 (300) |
| 23 | 10 | 560 (566) | 380 (466) | 100 (311) | 80 (300) |
| 23 | 15 | 800 (700) | 560 (566) | 140 (333) | 90 (305) |
| 23 | 20 | 1060 (844) | 740 (666) | 200 (366) | 100 (311) |
| 23 | 25 | 1160 (901) | 850 (727) | 250 (394) | 110 (316) |
| 23 | 30 | 1150 (894) | 880 (744) | 300 (415) | 120 (322) |
| 23 | 35 | 1060 (844) | 840 (722) | 320 (433) | 130 (327) |
| 24 | 0 | 80 (300) | 80 (300) | 80 (300) | 80 (300) |
| 24 | 5 | 380 (466) | 200 (366) | 80 (300) | 80 (300) |
| 24 | 10 | 630 (605) | 380 (466) | 90 (305) | 80 (300) |
| 24 | 15 | 900 (755) | 550 (581) | 110 (316) | 80 (300) |
| 24 | 20 | 1130 (883) | 750 (672) | 140 (333) | 90 (305) |
| 24 | 25 | 1130 (883) | 800 (700) | 160 (340) | 100 (311) |
| 24 | 30 | 1120 (877) | 840 (722) | 200 (366) | 110 (316) |
| 24 | 35 | 950 (783) | 780 (689) | 240 (389) | 120 (322) |
| 25 | 0 | 80 (300) | 80 (300) | 80 (300) | 80 (300) |
| 25 | 5 | 400 (477) | 270 (405) | 80 (300) | 80 (300) |
| 25 | 10 | 630 (605) | 420 (489) | 100 (311) | 80 (300) |
| 25 | 15 | 880 (744) | 580 (577) | 130 (327) | 90 (305) |
| 25 | 20 | 1120 (877) | 750 (672) | 160 (344) | 100 (311) |
| 25 | 25 | 1210 (920) | 840 (722) | 220 (377) | 110 (316) |
| 25 | 30 | 1210 (920) | 870 (744) | 270 (405) | 120 (322) |
| 25 | 35 | 1110 (872) | 820 (711) | 310 (427) | 140 (333) |
| 26 | 0 | 80 (300) | 80 (300) | 80 (300) | 80 (300) |
| 26 | 5 | 300 (415) | 220 (377) | 130 (327) | 80 (300) |
| 26 | 10 | 500 (533) | 400 (477) | 220 (377) | 80 (300) |
| 26 | 15 | 750 (672) | 570 (572) | 320 (433) | 100 (311) |
| 26 | 20 | 1000 (811) | 760 (677) | 420 (489) | 130 (327) |
| 26 | 25 | 1230 (938) | 920 (766) | 520 (544) | 170 (350) |
| 26 | 30 | 1230 (938) | 990 (805) | 600 (589) | 220 (377) |
| 26 | 35 | 1200 (922) | 1000 (811) | 650 (616) | 260 (400) |
| 27 | 0 | 80 (300) | 80 (300) | 80 (300) | 80 (300) |
| 27 | 5 | 300 (422) | 240 (389) | 100 (311) | 80 (300) |
| 27 | 10 | 520 (544) | 430 (494) | 160 (344) | 80 (300) |
| 27 | 15 | 780 (689) | 630 (605) | 230 (383) | 90 (305) |
| 27 | 20 | 1000 (811) | 830 (716) | 300 (415) | 110 (316) |
| 27 | 25 | 1200 (922) | 1010 (816) | 400 (477) | 140 (333) |
| 27 | 30 | 1200 (922) | 1040 (833) | 460 (511) | 170 (350) |
| 27 | 35 | 1140 (889) | 1000 (811) | 490 (527) | 200 (366) |
| 28 | 0 | 80 (300) | 80 (300) | 80 (300) | 80 (300) |
| 28 | 5 | 300 (415) | 200 (366) | 140 (333) | 80 (300) |
| 28 | 10 | 520 (544) | 380 (466) | 240 (389) | 90 (305) |
| 28 | 15 | 780 (689) | 540 (555) | 370 (461) | 120 (322) |
| 28 | 20 | 1000 (811) | 720 (655) | 500 (533) | 170 (350) |
| 28 | 25 | 1220 (933) | 900 (755) | 620 (600) | 230 (383) |
| 28 | 30 | 1220 (933) | 960 (789) | 690 (639) | 290 (416) |
| 28 | 35 | 1200 (922) | 980 (800) | 700 (644) | 340 (444) |

TABLE IV.- Continued

CHORDWISE TEMPERATURE-TIME HISTORIES OF THE SPECIMENS

| Specimen number | Time, sec | Temperature, °F (°K) | | | |
|-----------------|-----------|----------------------|----------------|----------------|----------------|
| | | Thermocouple 2 | Thermocouple 3 | Thermocouple 4 | Thermocouple 5 |
| 29 | 0 | 80 (300) | 80 (300) | 80 (300) | 80 (300) |
| 29 | 5 | 310 (427) | 230 (383) | 150 (339) | 90 (305) |
| 29 | 10 | 530 (550) | 420 (489) | 270 (405) | 100 (311) |
| 29 | 15 | 770 (683) | 610 (594) | 420 (489) | 150 (339) |
| 29 | 20 | 1010 (816) | 820 (711) | 480 (522) | 170 (350) |
| 29 | 25 | 1210 (927) | 1000 (811) | 480 (522) | 190 (361) |
| 29 | 30 | 1210 (927) | 1030 (827) | 470 (576) | 200 (366) |
| 29 | 35 | 1180 (911) | 1010 (816) | 440 (500) | 220 (377) |
| 30 | 0 | 80 (300) | 80 (300) | 80 (300) | 80 (300) |
| 30 | 5 | 320 (433) | 220 (377) | 120 (322) | 80 (300) |
| 30 | 10 | 560 (566) | 400 (477) | 180 (355) | 90 (305) |
| 30 | 15 | 800 (700) | 580 (577) | 240 (389) | 100 (311) |
| 30 | 20 | 1020 (822) | 770 (683) | 300 (415) | 130 (327) |
| 30 | 25 | 1230 (938) | 950 (783) | 400 (477) | 170 (350) |
| 30 | 30 | 1220 (933) | 990 (805) | 490 (527) | 210 (372) |
| 30 | 35 | 1200 (922) | 1000 (811) | 540 (555) | 240 (389) |
| 31 | 0 | 80 (300) | 80 (300) | 80 (300) | 80 (300) |
| 31 | 5 | 320 (433) | 250 (394) | 90 (305) | 80 (300) |
| 31 | 10 | 590 (583) | 430 (494) | 120 (322) | 90 (305) |
| 31 | 15 | 820 (711) | 630 (605) | 140 (333) | 100 (311) |
| 31 | 20 | 1060 (844) | 800 (700) | 180 (355) | 100 (311) |
| 31 | 25 | 1200 (922) | 960 (789) | 230 (383) | 110 (316) |
| 31 | 30 | 1200 (922) | 990 (805) | 280 (411) | 120 (322) |
| 31 | 35 | 1120 (877) | 960 (789) | 320 (433) | 140 (333) |
| 32 | 0 | 80 (300) | 80 (300) | 80 (300) | 80 (300) |
| 32 | 5 | 300 (415) | 250 (394) | 120 (322) | 80 (300) |
| 32 | 10 | 560 (566) | 420 (489) | 200 (366) | 90 (305) |
| 32 | 15 | 800 (700) | 630 (605) | 280 (411) | 110 (316) |
| 32 | 20 | 1040 (833) | 830 (716) | 360 (455) | 140 (333) |
| 32 | 25 | 1220 (933) | 1000 (811) | 420 (489) | 190 (361) |
| 32 | 30 | 1220 (933) | 1040 (833) | 500 (533) | 210 (372) |
| 32 | 35 | 1190 (916) | 1020 (822) | 580 (577) | 240 (389) |
| 33 | 0 | 80 (300) | 80 (300) | 80 (300) | 80 (300) |
| 33 | 5 | 300 (415) | 200 (366) | 80 (300) | 80 (300) |
| 33 | 10 | 530 (550) | 380 (466) | 110 (316) | 80 (300) |
| 33 | 15 | 780 (689) | 560 (566) | 160 (344) | 90 (305) |
| 33 | 20 | 1000 (811) | 740 (666) | 220 (377) | 110 (316) |
| 33 | 25 | 1200 (922) | 940 (827) | 300 (415) | 140 (333) |
| 33 | 30 | 1190 (916) | 980 (800) | 360 (455) | 170 (350) |
| 33 | 35 | 1150 (894) | 1000 (811) | 410 (483) | 200 (366) |
| 34 | 0 | 80 (300) | 80 (300) | 80 (300) | 80 (300) |
| 34 | 5 | 380 (466) | 260 (400) | 140 (333) | 80 (300) |
| 34 | 10 | 600 (588) | 430 (494) | 270 (405) | 90 (305) |
| 34 | 15 | 850 (727) | 600 (588) | 400 (477) | 110 (316) |
| 34 | 20 | 1080 (855) | 780 (689) | 520 (544) | 150 (339) |
| 34 | 25 | 1220 (927) | 940 (827) | 640 (611) | 200 (366) |
| 34 | 30 | 1210 (933) | 980 (800) | 690 (639) | 230 (383) |
| 34 | 35 | 1120 (877) | 970 (794) | 700 (644) | 240 (389) |

TABLE IV.— Continued

CHORDWISE TEMPERATURE-TIME HISTORIES OF THE SPECIMENS

| Specimen number | Time, sec | Temperature, °F (°K) | | | |
|-----------------|-----------|----------------------|----------------|----------------|----------------|
| | | Thermocouple 2 | Thermocouple 3 | Thermocouple 4 | Thermocouple 5 |
| 35 | 0 | 80 (300) | 80 (300) | 80 (300) | 80 (300) |
| 35 | 5 | 330 (439) | 220 (377) | 120 (322) | 80 (300) |
| 35 | 10 | 600 (588) | 220 (377) | 120 (322) | 80 (300) |
| 35 | 15 | 840 (722) | 380 (466) | 180 (355) | 100 (311) |
| 35 | 20 | 1100 (866) | 560 (566) | 240 (389) | 120 (322) |
| 35 | 25 | 1220 (933) | 760 (677) | 320 (433) | 160 (344) |
| 35 | 30 | 1220 (933) | 860 (739) | 400 (477) | 180 (355) |
| 35 | 35 | 1160 (900) | 890 (750) | 480 (522) | 240 (389) |
| 36 | 0 | 80 (300) | 80 (300) | 80 (300) | 80 (300) |
| 36 | 5 | 380 (466) | 290 (416) | 200 (366) | 130 (327) |
| 36 | 10 | 640 (611) | 470 (516) | 320 (433) | 200 (366) |
| 36 | 15 | 900 (755) | 700 (644) | 460 (511) | 280 (411) |
| 36 | 20 | 1140 (889) | 900 (755) | 600 (589) | 360 (455) |
| 36 | 25 | 1200 (922) | 1000 (811) | 700 (644) | 420 (489) |
| 36 | 30 | 1200 (922) | 1040 (833) | 760 (677) | 480 (522) |
| 36 | 35 | 1050 (839) | 960 (789) | 740 (666) | 480 (522) |
| 37 | 0 | 80 (300) | 80 (300) | 80 (300) | 80 (300) |
| 37 | 5 | 370 (461) | 230 (388) | 190 (361) | 80 (300) |
| 37 | 10 | 610 (594) | 370 (461) | 270 (405) | 80 (300) |
| 37 | 15 | 870 (744) | 510 (539) | 360 (455) | 80 (300) |
| 37 | 20 | 1130 (883) | 680 (633) | 450 (505) | 90 (305) |
| 37 | 25 | 1380 (1022) | 890 (750) | 580 (577) | 100 (311) |
| 37 | 30 | 1630 (1161) | 1100 (866) | 740 (666) | 120 (322) |
| 37 | 35 | 1690 (1194) | 1230 (938) | 820 (711) | 150 (339) |
| 37 | 40 | 1690 (1194) | 1300 (977) | 890 (750) | 190 (361) |
| 37 | 45 | 1540 (1111) | 1230 (938) | 860 (739) | 220 (377) |
| 37 | 50 | 1400 (1033) | 1170 (905) | 830 (716) | 240 (389) |
| 38 | 0 | 80 (300) | 80 (300) | 80 (300) | 80 (300) |
| 38 | 5 | 320 (433) | 200 (366) | 160 (344) | 80 (300) |
| 38 | 10 | 600 (589) | 340 (444) | 230 (383) | 80 (300) |
| 38 | 15 | 880 (744) | 500 (533) | 310 (427) | 90 (305) |
| 38 | 20 | 1150 (894) | 680 (633) | 400 (477) | 110 (316) |
| 38 | 25 | 1400 (1033) | 870 (744) | 500 (533) | 120 (322) |
| 38 | 30 | 1630 (1161) | 1100 (866) | 630 (605) | 150 (339) |
| 38 | 35 | 1720 (1211) | 1240 (944) | 720 (655) | 190 (361) |
| 38 | 40 | 1720 (1211) | 1320 (989) | 770 (683) | 230 (383) |
| 38 | 45 | 1530 (1005) | 1260 (955) | 730 (661) | 260 (400) |
| 38 | 50 | 1360 (1011) | 1180 (911) | 710 (649) | 290 (416) |
| 39 | 0 | 80 (300) | 80 (300) | 80 (300) | 80 (300) |
| 39 | 5 | 400 (477) | 210 (372) | 170 (350) | 80 (300) |
| 39 | 10 | 660 (622) | 350 (450) | 250 (394) | 80 (300) |
| 39 | 15 | 930 (772) | 510 (539) | 340 (444) | 100 (311) |
| 39 | 20 | 1200 (922) | 710 (649) | 430 (494) | 120 (322) |
| 39 | 25 | 1480 (1077) | 930 (772) | 590 (583) | 140 (333) |
| 39 | 30 | 1710 (1205) | 1170 (905) | 770 (683) | 180 (355) |
| 39 | 35 | 1700 (1200) | 1250 (950) | 850 (727) | 210 (372) |
| 39 | 40 | 1600 (1144) | 1230 (938) | 900 (755) | 250 (394) |
| 39 | 45 | 1350 (1005) | 1100 (866) | 830 (716) | 280 (411) |
| 39 | 50 | 1180 (911) | 1000 (811) | 796 (694) | 300 (415) |

TABLE IV.- Continued

CHORDWISE TEMPERATURE-TIME HISTORIES OF THE SPECIMENS

| Specimen number | Time, sec | Temperature, °F (°K) | | | |
|--------------------|--------------|----------------------|----------------|----------------|----------------|
| | | Thermocouple 2 | Thermocouple 3 | Thermocouple 4 | Thermocouple 5 |
| 40 | 0 | 80 (300) | 80 (300) | 80 (300) | 80 (300) |
| 40 | 5 | 360 (455) | 200 (366) | 100 (311) | 80 (300) |
| 40 | 10 | 610 (494) | 320 (433) | 130 (327) | 80 (300) |
| 40 | 15 | 880 (744) | 480 (522) | 200 (366) | 100 (311) |
| 40 | 20 | 1130 (938) | 650 (616) | 270 (405) | 110 (316) |
| 40 | 25 | 1400 (1033) | 850 (727) | 360 (455) | 130 (327) |
| 40 | 30 | 1640 (1166) | 1080 (855) | 450 (505) | 160 (344) |
| 40 | 35 | 1710 (1205) | 1270 (961) | 580 (577) | 210 (372) |
| 40 | 40 | 1710 (1205) | 1350 (1005) | 650 (616) | 240 (389) |
| 40 | 45 | 1470 (1072) | 1290 (972) | 680 (633) | 270 (405) |
| 40 | 50 | 1240 (944) | 1160 (900) | 640 (611) | 290 (416) |
| 41 | 0 | 80 (300) | 80 (300) | 80 (300) | 80 (300) |
| 41 | 5 | 350 (450) | 260 (400) | 130 (327) | 80 (300) |
| 41 | 10 | 620 (600) | 430 (494) | 200 (366) | 80 (300) |
| 41 | 15 | 890 (750) | 610 (594) | 260 (400) | 110 (316) |
| 41 | 20 | 1140 (889) | 800 (700) | 330 (439) | 130 (327) |
| 41 | 25 | 1400 (1033) | 1000 (811) | 430 (494) | 170 (350) |
| 41 | 30 | 1650 (1172) | 1220 (933) | 570 (572) | 220 (377) |
| 41 | 35 | 1700 (1200) | 1320 (989) | 660 (672) | 280 (411) |
| 41 | 40 | 1700 (1200) | 1370 (1016) | 720 (655) | 310 (427) |
| 41 | 45 | 1430 (1050) | 1190 (916) | 690 (639) | 330 (439) |
| 41 | 50 | 1190 (916) | 1020 (822) | 640 (611) | 340 (444) |
| 42 | 0 | 80 (300) | 80 (300) | 80 (300) | 80 (300) |
| 42 | 5 | 380 (466) | 240 (389) | 80 (300) | 80 (300) |
| 42 | 10 | 630 (605) | 400 (477) | 100 (311) | 80 (300) |
| 42 | 15 | 920 (766) | 580 (577) | 120 (322) | 80 (300) |
| 42 | 20 | 1200 (922) | 770 (688) | 170 (350) | 100 (311) |
| 42 | 25 | 1460 (1066) | 990 (805) | 230 (383) | 110 (316) |
| 42 | 30 | 1680 (1189) | 1230 (938) | 320 (433) | 130 (327) |
| 42 | 35 | 1760 (1233) | 1350 (1005) | 410 (483) | 160 (344) |
| 42 | 40 | 1730 (1216) | 1400 (1033) | 480 (522) | 190 (361) |
| 42 | 45 | 1490 (1083) | 1260 (955) | 520 (544) | 210 (372) |
| 42 | 50 | 1270 (961) | 1120 (877) | 540 (555) | 220 (377) |
| 43 | 0 | 80 (300) | 80 (300) | 80 (300) | 80 (300) |
| 43 | 5 | 350 (450) | 210 (372) | 120 (322) | 80 (300) |
| 43 | 10 | 620 (600) | 370 (461) | 180 (355) | 80 (300) |
| 43 | 15 | 920 (766) | 530 (550) | 240 (389) | 100 (311) |
| 43 | 20 | 1200 (922) | 720 (655) | 310 (427) | 140 (333) |
| 43 | 25 | 1460 (1066) | 910 (761) | 400 (477) | 200 (366) |
| 43 | 30 | 1700 (1200) | 1120 (877) | 500 (533) | 260 (400) |
| 43 | 35 | 1740 (1222) | 1200 (922) | 600 (589) | 320 (453) |
| 43 | 40 | 1720 (1211) | 1240 (944) | 670 (629) | 380 (466) |
| 43 | 45 | 1330 (994) | 1030 (827) | 630 (605) | 390 (472) |
| 43 | 50 | 1000 (811) | 820 (711) | 560 (566) | 370 (461) |

TABLE IV.- Continued

CHORDWISE TEMPERATURE-TIME HISTORIES OF THE SPECIMENS

| Specimen number | Time, sec | Temperature, °F (°K) | | | |
|-----------------|-----------|----------------------|----------------|----------------|----------------|
| | | Thermocouple 2 | Thermocouple 3 | Thermocouple 4 | Thermocouple 5 |
| 44 | 0 | 80 (300) | 80 (300) | 80 (300) | 80 (300) |
| 44 | 5 | 360 (455) | 220 (377) | 80 (300) | 80 (300) |
| 44 | 10 | 620 (600) | 350 (450) | 80 (300) | 80 (300) |
| 44 | 15 | 890 (750) | 500 (533) | 100 (311) | 90 (305) |
| 44 | 20 | 1150 (894) | 670 (627) | 130 (327) | 120 (322) |
| 44 | 25 | 1400 (1033) | 830 (716) | 200 (366) | 150 (339) |
| 44 | 30 | 1650 (1172) | 1050 (839) | 290 (416) | 200 (366) |
| 44 | 35 | 1690 (1194) | 1190 (916) | 420 (489) | 230 (383) |
| 44 | 40 | 1690 (1194) | 1260 (955) | 510 (539) | 270 (405) |
| 44 | 45 | 1320 (989) | 1080 (855) | 590 (583) | 280 (411) |
| 44 | 50 | 1010 (816) | 870 (744) | 570 (572) | 290 (416) |
| 45 | 0 | 80 (300) | 80 (300) | 80 (300) | 80 (300) |
| 45 | 5 | 350 (450) | 240 (389) | 80 (300) | 80 (300) |
| 45 | 10 | 650 (639) | 400 (477) | 110 (316) | 80 (300) |
| 45 | 15 | 970 (794) | 590 (583) | 170 (350) | 110 (316) |
| 45 | 20 | 1270 (961) | 800 (700) | 230 (383) | 130 (327) |
| 45 | 25 | 1540 (1111) | 1050 (839) | 330 (439) | 180 (355) |
| 45 | 30 | 1780 (1244) | 1300 (977) | 450 (505) | 240 (389) |
| 45 | 35 | 1760 (1233) | 1400 (1033) | 610 (539) | 300 (415) |
| 45 | 40 | 1650 (1172) | 1300 (977) | 720 (655) | 340 (444) |
| 45 | 45 | 1220 (933) | 1060 (844) | 760 (677) | 350 (450) |
| 45 | 50 | 920 (766) | 880 (744) | 670 (627) | 350 (450) |
| 46 | 0 | 80 (300) | 80 (300) | 80 (300) | 80 (300) |
| 46 | 5 | 370 (461) | 220 (377) | 180 (355) | 80 (300) |
| 46 | 10 | 610 (394) | 370 (461) | 230 (383) | 80 (300) |
| 46 | 15 | 870 (744) | 530 (550) | 320 (433) | 110 (316) |
| 46 | 20 | 1130 (883) | 720 (655) | 420 (489) | 150 (339) |
| 46 | 25 | 1380 (1022) | 920 (766) | 580 (577) | 210 (372) |
| 46 | 30 | 1630 (1161) | 1170 (905) | 740 (666) | 290 (416) |
| 46 | 35 | 1710 (1205) | 1290 (972) | 860 (739) | 360 (455) |
| 46 | 40 | 1710 (1205) | 1360 (1011) | 950 (783) | 420 (489) |
| 46 | 45 | 1370 (1016) | 1160 (900) | 830 (716) | 420 (489) |
| 46 | 50 | 1020 (822) | 930 (772) | 720 (655) | 410 (483) |
| 47 | 0 | 80 (300) | 80 (300) | 80 (300) | 80 (300) |
| 47 | 5 | 380 (466) | 230 (383) | 100 (311) | 80 (300) |
| 47 | 10 | 640 (611) | 400 (477) | 130 (327) | 90 (305) |
| 47 | 15 | 930 (772) | 600 (588) | 180 (355) | 110 (316) |
| 47 | 20 | 1220 (933) | 820 (711) | 240 (389) | 130 (327) |
| 47 | 25 | 1450 (1061) | 1050 (839) | 360 (455) | 170 (350) |
| 47 | 30 | 1580 (1133) | 1230 (938) | 480 (522) | 210 (372) |
| 47 | 35 | 1650 (1172) | 1370 (1016) | 590 (583) | 260 (400) |
| 47 | 40 | 1680 (1189) | 1460 (1066) | 690 (639) | 290 (416) |
| 47 | 45 | 1510 (1094) | 1440 (1055) | 720 (655) | 310 (427) |
| 47 | 50 | 1280 (966) | 1260 (955) | 710 (649) | 330 (439) |

TABLE IV.- Concluded

CHORDWISE TEMPERATURE-TIME HISTORIES OF THE SPECIMENS

| Specimen number | Time, sec | Temperature, °F (°K) | | | |
|-----------------|-----------|----------------------|----------------|----------------|----------------|
| | | Thermocouple 2 | Thermocouple 3 | Thermocouple 4 | Thermocouple 5 |
| 48 | 0 | 80 (300) | 80 (300) | 80 (300) | 80 (300) |
| 48 | 5 | 370 (461) | 200 (366) | 100 (311) | 80 (300) |
| 48 | 10 | 650 (639) | 360 (455) | 110 (316) | 80 (300) |
| 48 | 15 | 930 (772) | 550 (561) | 120 (322) | 100 (311) |
| 48 | 20 | 1220 (933) | 770 (683) | 150 (339) | 110 (316) |
| 48 | 25 | 1480 (1077) | 980 (800) | 200 (366) | 120 (322) |
| 48 | 30 | 1700 (1200) | 1210 (927) | 250 (394) | 140 (333) |
| 48 | 35 | 1730 (1216) | 1390 (1027) | 320 (433) | 170 (350) |
| 48 | 40 | 1720 (1211) | 1460 (1066) | 420 (489) | 200 (366) |
| 48 | 45 | 1330 (994) | 1270 (961) | 480 (522) | 230 (383) |
| 48 | 50 | 1020 (822) | 1030 (827) | 510 (539) | 240 (389) |
| 49 | 0 | 80 (300) | 80 (300) | 80 (300) | 80 (300) |
| 49 | 5 | 350 (450) | 250 (394) | 120 (322) | 80 (300) |
| 49 | 10 | 640 (611) | 400 (477) | 180 (355) | 100 (311) |
| 49 | 15 | 920 (766) | 570 (572) | 250 (394) | 120 (322) |
| 49 | 20 | 1200 (922) | 750 (672) | 320 (433) | 140 (333) |
| 49 | 25 | 1470 (1072) | 930 (772) | 400 (477) | 160 (344) |
| 49 | 30 | 1720 (1211) | 1160 (900) | 490 (527) | 190 (361) |
| 49 | 35 | 1760 (1233) | 1300 (977) | 630 (605) | 230 (383) |
| 49 | 40 | 1740 (1222) | 1380 (1022) | 760 (677) | 270 (405) |
| 49 | 45 | 1520 (1100) | 1150 (894) | 760 (677) | 280 (411) |
| 49 | 50 | 1320 (989) | 920 (766) | 680 (633) | 280 (411) |
| 50 | 0 | 80 (300) | 80 (300) | 80 (300) | 80 (300) |
| 50 | 5 | 350 (450) | 230 (383) | 170 (350) | 80 (300) |
| 50 | 10 | 640 (611) | 390 (472) | 240 (389) | 90 (305) |
| 50 | 15 | 920 (766) | 580 (577) | 330 (439) | 100 (311) |
| 50 | 20 | 1200 (922) | 770 (683) | 430 (494) | 130 (327) |
| 50 | 25 | 1470 (1072) | 980 (800) | 570 (572) | 170 (350) |
| 50 | 30 | 1720 (1211) | 1200 (922) | 720 (655) | 220 (377) |
| 50 | 35 | 1760 (1233) | 1320 (989) | 820 (711) | 270 (405) |
| 50 | 40 | 1740 (1222) | 1380 (1022) | 900 (755) | 280 (411) |
| 50 | 45 | 1520 (1100) | 1280 (966) | 890 (750) | 300 (422) |
| 50 | 50 | 1320 (989) | 1160 (900) | 850 (727) | 320 (433) |
| 51 | 0 | 80 (300) | 80 (300) | 80 (300) | 80 (300) |
| 51 | 5 | 360 (455) | 230 (383) | 90 (305) | 80 (300) |
| 51 | 10 | 620 (600) | 360 (455) | 100 (311) | 80 (300) |
| 51 | 15 | 890 (750) | 500 (533) | 110 (316) | 100 (311) |
| 51 | 20 | 1150 (894) | 630 (605) | 140 (333) | 120 (322) |
| 51 | 25 | 1400 (1033) | 810 (705) | 180 (355) | 130 (327) |
| 51 | 30 | 1660 (1177) | 1000 (811) | 230 (383) | 150 (339) |
| 51 | 35 | 1700 (1200) | 1100 (866) | 290 (416) | 170 (350) |
| 51 | 40 | 1700 (1200) | 1170 (905) | 330 (439) | 180 (355) |
| 51 | 45 | 1500 (1089) | 1080 (855) | 380 (466) | 190 (361) |
| 51 | 50 | 1300 (977) | 990 (805) | 390 (472) | 200 (366) |

"The aeronautical and space activities of the United States shall be conducted so as to contribute . . . to the expansion of human knowledge of phenomena in the atmosphere and space. The Administration shall provide for the widest practicable and appropriate dissemination of information concerning its activities and the results thereof."

—NATIONAL AERONAUTICS AND SPACE ACT OF 1958

NASA SCIENTIFIC AND TECHNICAL PUBLICATIONS

TECHNICAL REPORTS: Scientific and technical information considered important, complete, and a lasting contribution to existing knowledge.

TECHNICAL NOTES: Information less broad in scope but nevertheless of importance as a contribution to existing knowledge.

TECHNICAL MEMORANDUMS: Information receiving limited distribution because of preliminary data, security classification, or other reasons.

CONTRACTOR REPORTS: Technical information generated in connection with a NASA contract or grant and released under NASA auspices.

TECHNICAL TRANSLATIONS: Information published in a foreign language considered to merit NASA distribution in English.

TECHNICAL REPRINTS: Information derived from NASA activities and initially published in the form of journal articles.

SPECIAL PUBLICATIONS: Information derived from or of value to NASA activities but not necessarily reporting the results of individual NASA-programmed scientific efforts. Publications include conference proceedings, monographs, data compilations, handbooks, sourcebooks, and special bibliographies.

Details on the availability of these publications may be obtained from:

SCIENTIFIC AND TECHNICAL INFORMATION DIVISION
NATIONAL AERONAUTICS AND SPACE ADMINISTRATION

Washington, D.C. 20546